Previous Page

Scenario 3: Effect of the JFK Causeway

The purpose of Scenario 3 is to examine the effect of the JFK Causeway by removing it from the model. Figure IV.18 shows the computational grid for the Flour Bluff area used in the scenario. The JFK Causeway, which is the shaded area in the figure, is replaced by computational elements for free water flow.

Table IV.9 lists the monthly average salinity differences between the existing and the causeway removal case for the 1988-1989 and 1991-1992 simulations. Figures IV.19(a) through IV.19(f) for 1988-1989 and Figures IV.20(a) through IV.20(f) for 1991-1992 are the time histories of scenario salinities at selected locations compared with the existing condition. Figure IV.21 is a plot of salinity differences for August 1989 and Figure IV.22 for May 1992.

The patterns of existing and scenario salinities in Figures IV.19 and IV.20 at all sites are nearly identical. Contrary to expectations, the effect of JFK Causeway removal appears to be minimal. Salinity at the JFK Causeway site during the dry period of 1989 is as much as 0.9‰ higher than the existing condition, but higher by no more than 0.4‰ in the wet period of 1992. The increased salinity during the 1989 dry period is probably due to increased flows from the south despite increased flows from Corpus Christi Bay. The additional flow from the south increases the salinity more than the additional flow from the north reduces it.

Table IV.10 lists the average daily flows in the JFK Causeway area and Figure IV.23 displays those flows. In the dry year, the flows to the south at the NAS-GIWW section increase only 4% (8.66/8.36=1.036) for the 1988-1989 simulation. The magnitude of the additional flow to the south (8.66-8.36=0.30) is approximately equal to the additional flow to the north (5.06-4.77=0.29), but the higher salinity of the water from the south results in a net salinity increase. The small volume of increased flows to the Laguna Madre is the reason the salinity change is small.

In the wet year, the flows to the south at the NAS-GIWW section increase about 4% (8.20/7.86=1.043) for the 1991-1992 simulation. The volume of the additional flow to the south (8.20-7.86=0.34) is about 40% (0.34/0.25=1.36) larger than the additional flow to the north (5.61-5.36=0.25). As a result, the larger volume of higher salinity water from the north slightly increases the salinity. Flows across the Humble-JFK section for the removal scenario do not include the elevated portion because it is difficult to compute flows after the causeway is removed at this section.

Table IV.9 Salinity differences between the existing condition and JFK Causeway removal. The difference is positive if the existing salinity is higher than the simulated salinity

Year	Month	Aransas Bay	Nueces Bay	Corpus Bay	Naval Air Sta.	GIWW JFK	GIWW Pita	Baffin Bay
1988	1	0.00	-0.02	-0.03	-0.05	-0.04	-0.02	0.00
1988	2	0.00	-0.07	-0.05	-0.07	-0.08	-0.06	-0.01
1988	3	0.00	-0.10	-0.05	-0.11	-0.11	-0.08	-0.01
1988	4	0.00	-0.10	-0.05	-0.10	-0.11	-0.10	-0.02
1988	5	0.00	-0.09	-0.04	-0.09	-0.12	-0.08	-0.04
1988	6	0.01	-0.08	-0.03	-0.07	-0.08	-0.06	-0.05
1988	7	0.01	-0.08	-0.03	-0.16	-0.22	-0.06	-0.06
1988	8	0.01	-0.05	-0.02	-0.12	-0.25	-0.12	-0.04
1988	9	0.01	-0.04	-0.01	-0.04	-0.05	-0.03	-0.04
1988	10	0.00	-0.13	-0.07	-0.13	-0.15	-0.10	-0.03
1988	11	0.00	-0.14	-0.07	-0.16	-0.19	-0.13	-0.03
1988	12	-0.01	-0.13	-0.07	-0.16	-0.21	-0.14	-0.04
1989	1	0.00	-0.13	-0.07	-0.14	-0.16	-0.14	-0.06
1989	2	0.00	-0.13	-0.07	-0.15	-0.15	-0.13	-0.11
1989	3	0.00	-0.13	-0.07	-0.15	-0.18	-0.14	-0.11
1989	4	0.00	-0.11	-0.06	-0.15	-0.21	-0.17	-0.09
1989	5	0.00	-0.11	-0.06	-0.31	-0.44	-0.19	-0.10
1989	6	0.00	-0.01	-0.02	-0.45	-0.93	-0.31	-0.11
1989	7	0.01	0.03	0.02	-0.23	-0.56	-0.26	-0.13
1989	8	0.01	0.06	0.04	-0.01	-0.11	-0.04	-0.13
1989	9	0.01	0.01	0.01	-0.01	-0.03	0.02	0.04
1989	10	0.00	-0.05	-0.03	-0.07	-0.08	-0.04	-0.01
1989	11	0.01	-0.08	-0.03	-0.09	-0.10	-0.06	-0.03
1989	12	0.00	-0.10	-0.07	-0.13	-0.13	-0.10	-0.06
1991	5	0.00	-0.04	-0.05	-0.11	-0.14	-0.08	-0.01
1991	6	0.01	-0.13	-0.09	-0.23	-0.26	-0.08	-0.01
1991	7	0.00	-0.12	-0.10	-0.42	-0.47	-0.04	0.00
1991	8	-0.01	-0.06	-0.07	-0.40	-0.60	-0.14	0.00
1991	9	0.00	-0.08	-0.05	-0.11	-0.14	-0.15	-0.01
1991	10	0.00	-0.12	-0.07	-0.14	-0.16	-0.13	-0.10
1991	11	0.02	-0.14	-0.08	-0.18	-0.20	-0.15	-0.11
1991	12	0.02	-0.11	-0.07	-0.15	-0.19	-0.19	-0.10
1992	1	0.03	-0.08	-0.09	-0.14	-0.11	-0.12	-0.11
1992	2	0.03	-0.04	-0.13	-0.20	-0.19	-0.14	-0.05
1992	3	0.01	-0.05	-0.12	-0.17	-0.21	-0.16	-0.05
1992	4	0.04	-0.07	-0.14	-0.18	-0.14	-0.16	-0.06
1992	5	0.03	-0.09	-0.18	-0.20	-0.14	-0.13	-0.06
1992	6	0.04	-0.04	-0.17	-0.22	-0.21	-0.09	-0.06
1992	7	-0.02	-0.03	-0.11	-0.31	-0.35	-0.10	-0.07
1992	8	-0.02	-0.11	-0.13	-0.26	-0.28	-0.18	-0.08
1992	9	-0.01	-0.21	-0.15	-0.20	-0.19	-0.20	-0.08
1992	10	-0.01	-0.23	-0.14	-0.22	-0.22	-0.23	-0.14
1992	11	0.00	-0.20	-0.12	-0.21	-0.21	-0.22	-0.16

The Pita-GIWW cross section does not show much salinity change under wet or dry years. In wet years, the north and south flows balance; in the dry years, the average daily flow to the south is about 1% greater, while the flow to the north increases about 4%. However, this increased flow of the higher salinity water from the south is not great enough to significantly change the salinity.

Table IV.10 Average daily flows (1000 ac-ft) through cross-sections.
In means flow to the south, out means flow to the north

Scenario	Simulation Year	In/Out	NAS-GIWW	Humble-JFK/GIWW	Pita-GIWW
Existing	1988-1989	In	8.36	9.30	7.63
Existing	1988-1989	Out	4.77	5.11	5.32
		Difference	3.59	4.19	2.31
JFK_Rmvd	1988-1989	In	8.66	4.85[a]	7.73
JFK_Rmvd	1988-1989	Out	5.06	2.76[a]	5.51
		Difference	3.60	2.09[a]	2.22
Existing	1991-1992	In	7.86	8.72	6.84
Existing	1991-1992	Out	5.36	5.98	6.48
		Difference	2.50	2.74	0.36
JFK_Rmvd	1991-1992	In	8.20	4.75[a]	6.99
JFK_Rmvd	1991-1992	Out	5.61	2.82[a]	6.66
		Difference	2.59	1.93[a]	0.33

a) These flows do not include the flow through the removed portion of the causeway

Figure IV.21 shows the spatial extent of the salinity differences with respect to JFK Causeway removal for the August 1989 simulation. Note that the scale of change is very small, only about 0.7‰ between the greatest positive and negative changes. Two areas would be affected by the removal, the Laguna Madre area and Oso Bay. Under the conditions in this figure, the scenario would cause a salinity increase at both locations. The increase in Oso Bay would be the result of the operation of the B. Davis Power Plant, which would pump water of slightly higher salinity (due to causeway removal) from Laguna Madre. The water would be discharged into Oso Bay, thereby increasing Oso Bay salinity.

Figure IV.22 shows the salinity differences in May 1992 for a wet period. As in the case of the dry period, the effect of causeway removal on salinity is limited in magnitude but more areas are shown to be affected. Corpus Christi Bay would be higher 0.2 to 0.4‰; Oso Bay would also be higher by 0.5‰ or less.

A previous study by Matsumoto (1991) indicated a 4 to 5% increase in flow exchange would occur under various alternatives for opening the causeway. This earlier conclusion is consistent with the current one. The differences between the previous study and this one are: (1) the model is an updated version of the previous model in which a new parameter was added to enforce mass conservation; (2) representation of the JFK Causeway area is more detailed; (3) flow exchanges are examined over a longer period and under different conditions; and (4) salinity changes are directly examined.

Brown et al. (1995) did not address salinity changes. Instead, they compared the flow velocities and extent of spatial change. They investigated the influence of the Barney Davis Power Plant operation on the circulation by simulating the case with and without the plant and compared the discharges through the causeway. It is somewhat puzzling that the power plant does not have a significant influence on the discharge through the causeway. Brown et al. stated that the total volume of water is basically unchanged because the Humble Channel and the GIWW are at nearly equilibrium depths that allow almost unimpeded flow. They closely examined the velocity differences and spatial extent of the changes under different alternative designs and different conditions such as summer, winter, weak wind, strong wind, and storm condition. Their model simulated periods of 14 to 30 days. They found that most velocities in the shallow portions of the causeway area are on the order of 5 cm/s (0.16 fps) and the velocity increase ranged from 1 to 4 cm/s, which is significant in terms of the percentage increase (25% to 80%). Their recommendation was in line with Duke's recommendation (1991) that the best place to open the causeway is on the west side of the Humble Channel. In part, Duke's recommendation was based on historical information indicating deeper water along the mainland shoreline.

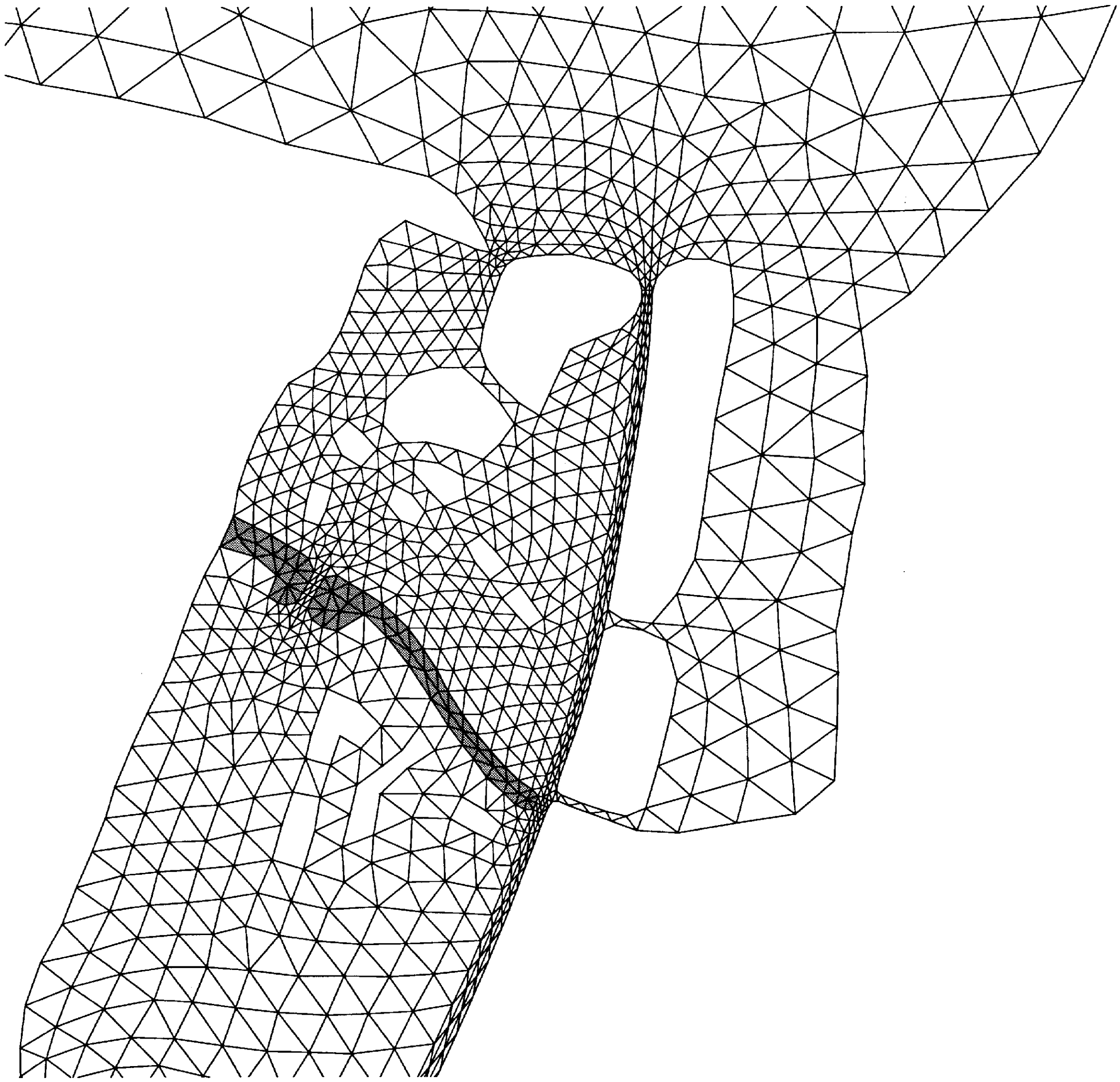

Figure IV.18 Computational grid, focussing on Flour Bluff area, for the JFK Causeway removal case; the shaded elements represent the elevated Causeway elements

(a) Mid Nueces Bay

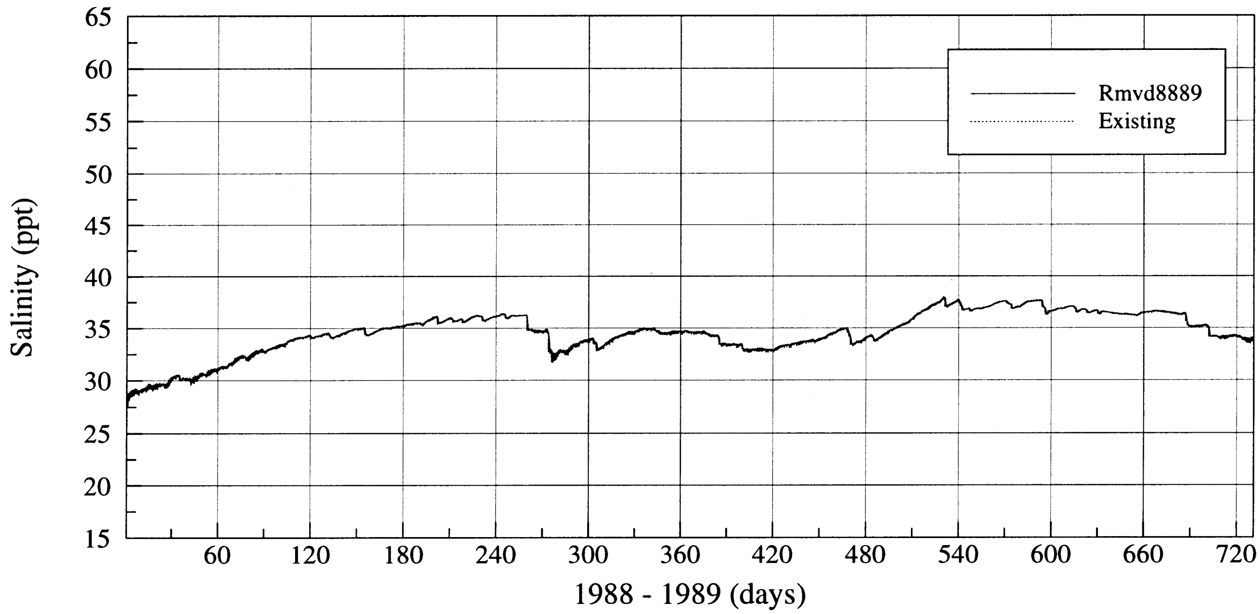

(b) Mid Corpus Christi Bay

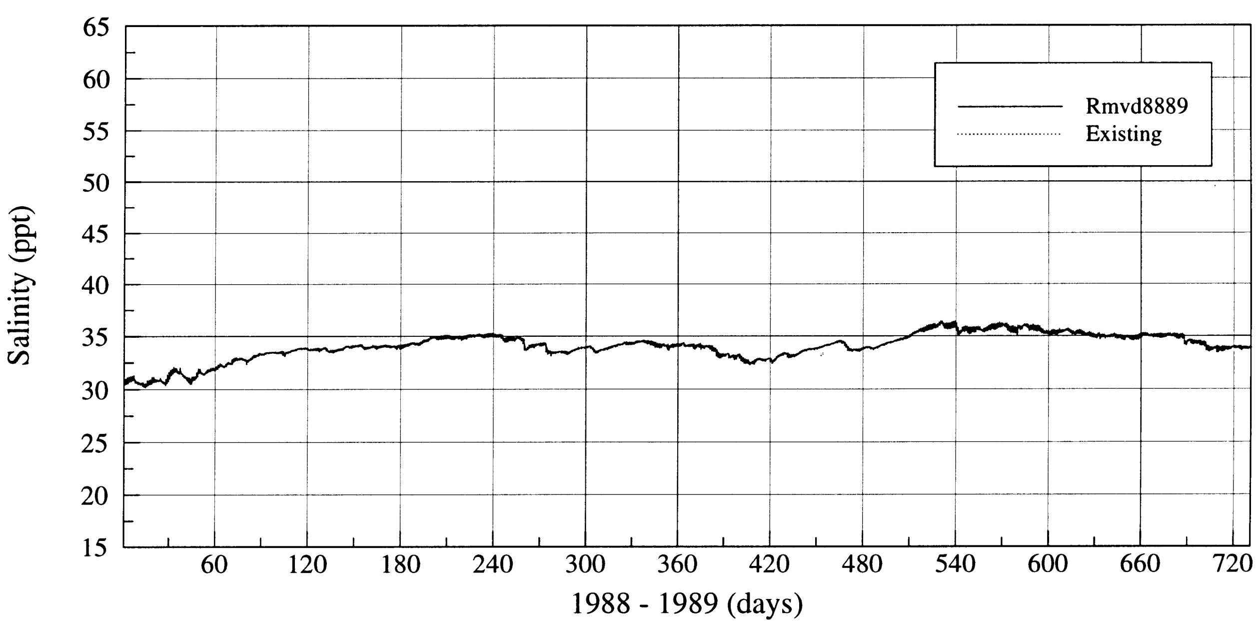

Figure IV.19 Simulated salinities in 1988-1989 for the existing condition and for the JFK Causeway removal scenario

(c) JFK Causeway

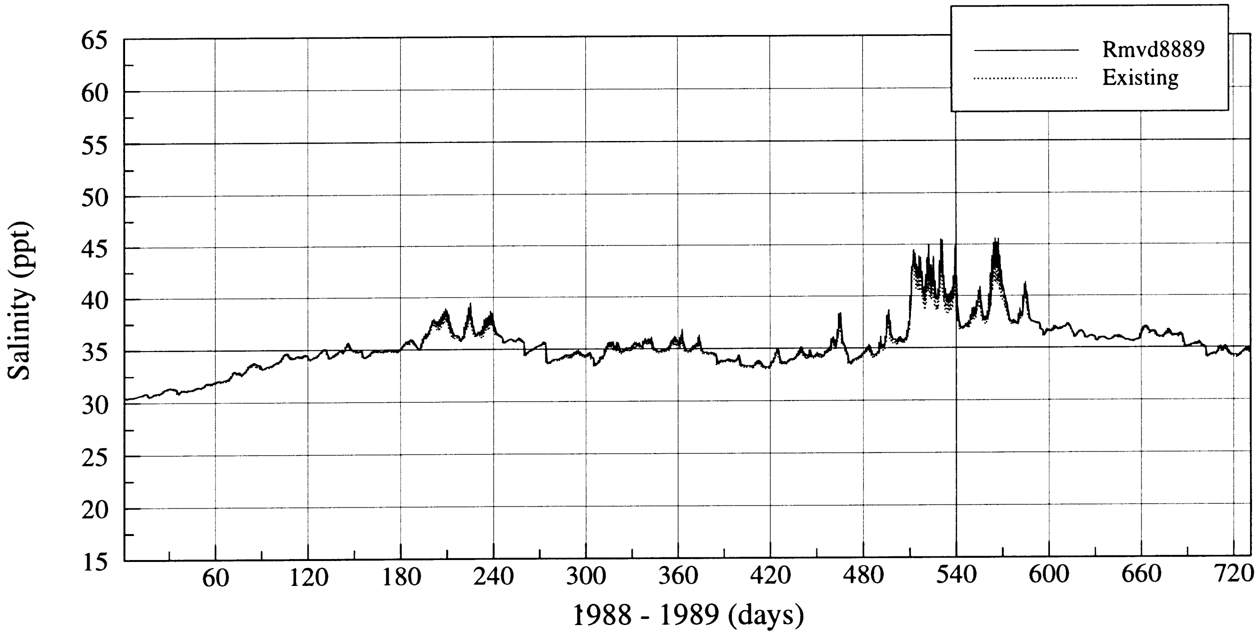

(d) Naval Air Station

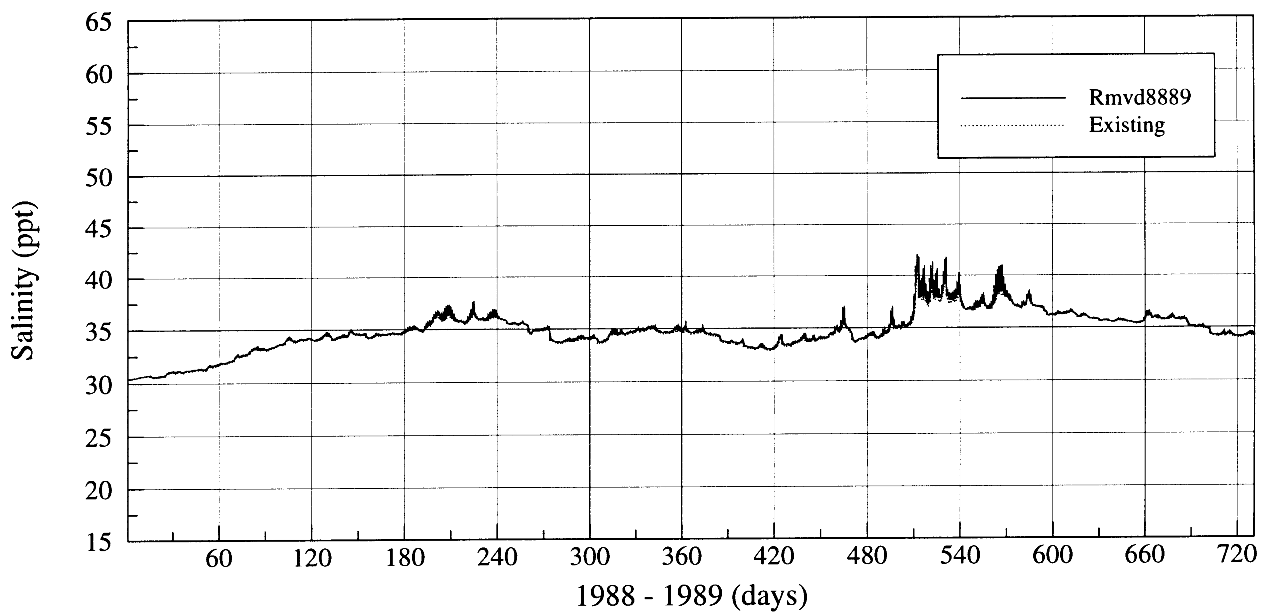

Figure IV.19 Simulated salinities in 1988-1989 for the existing condition and for the JFK Causeway removal scenario

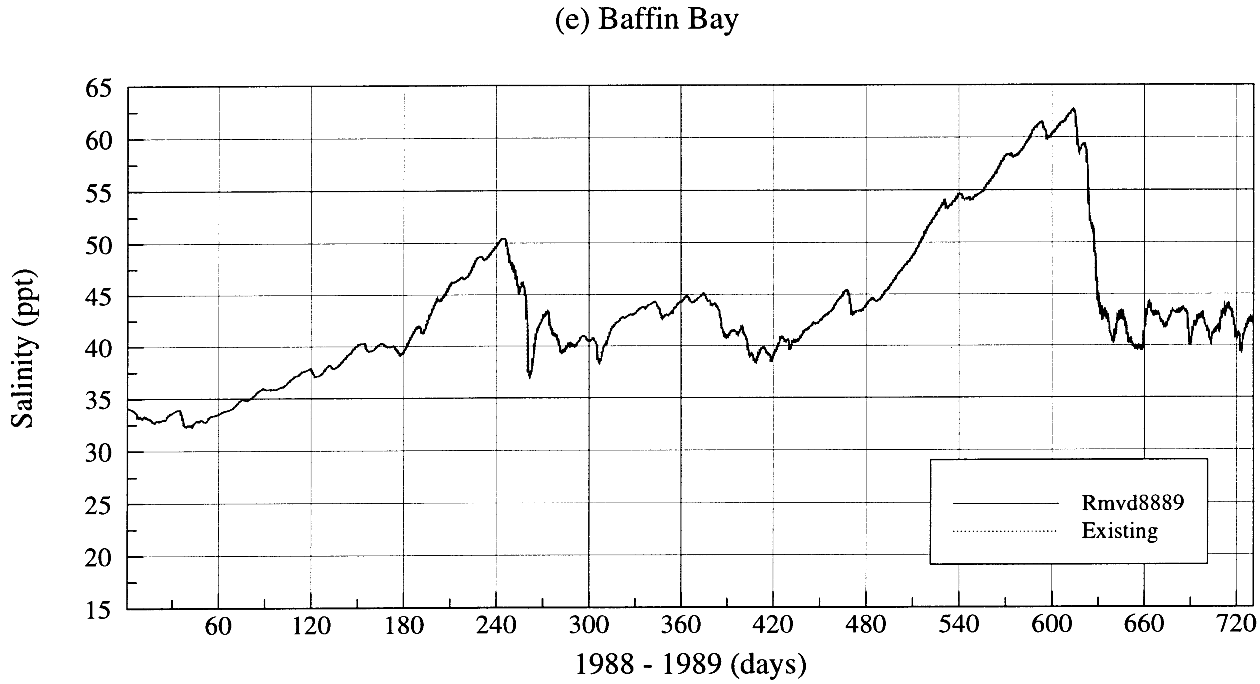

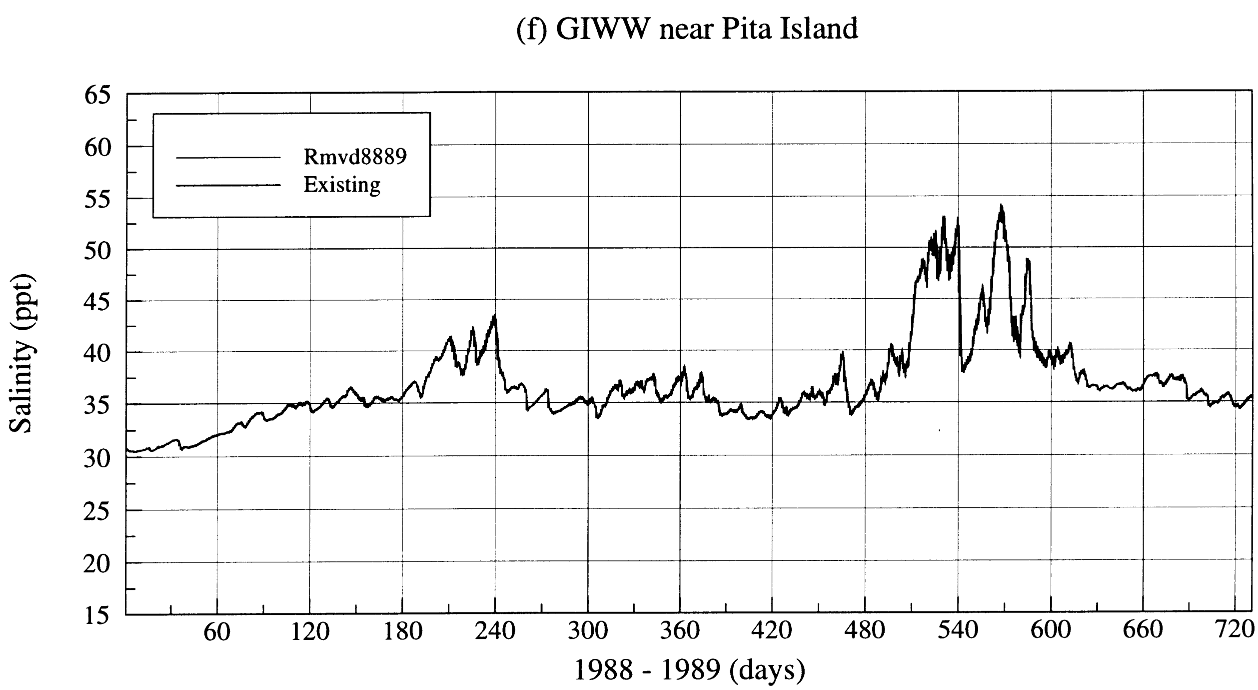

Figure IV.19 Simulated salinities in 1988-1989 for the existing condition and for the JFK Causeway removal scenario

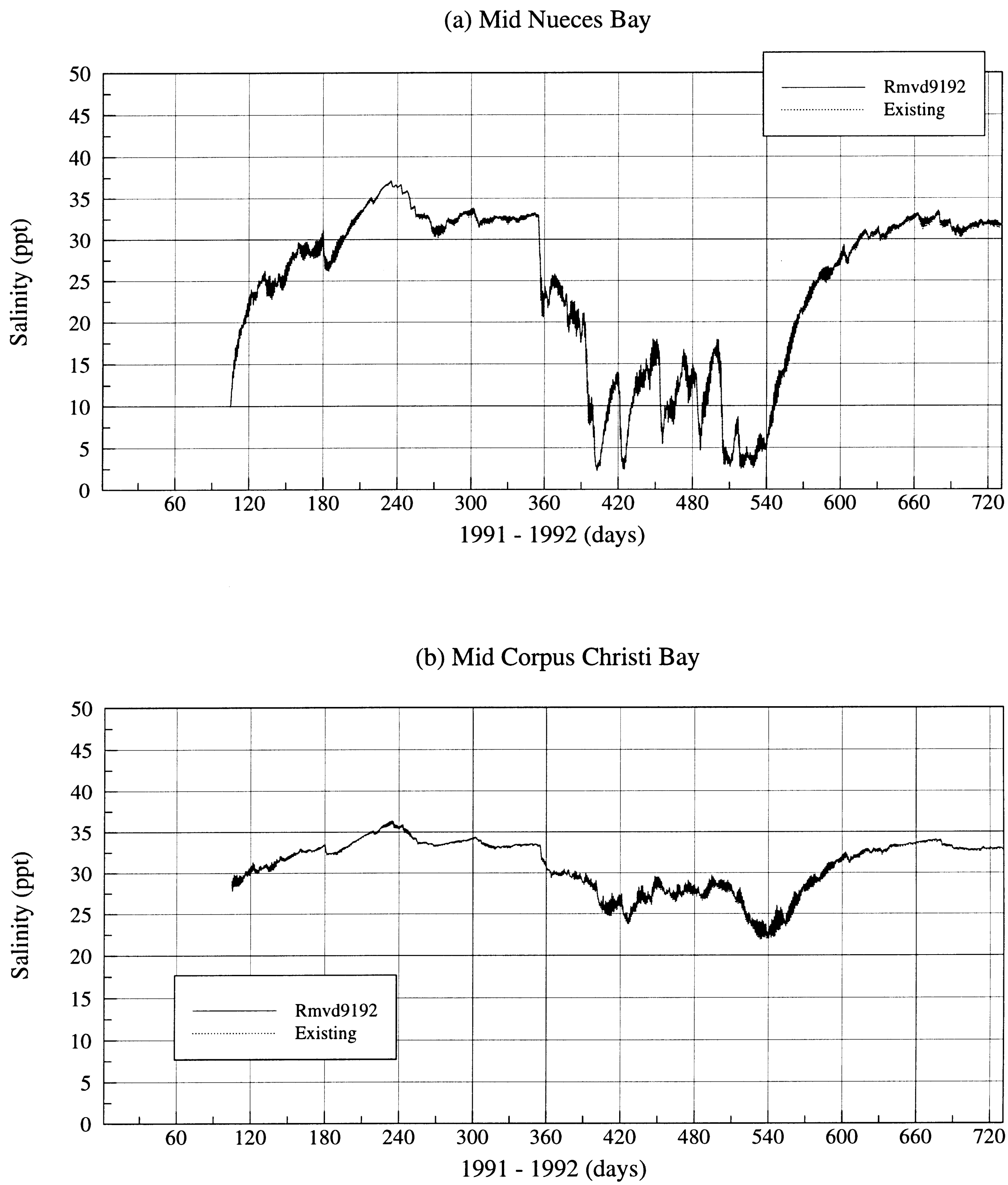

Figure IV.20 Simulated salinities in 1991-1992 for the existing condition and for the JFK Causeway removal scenario

(c) JFK Causeway

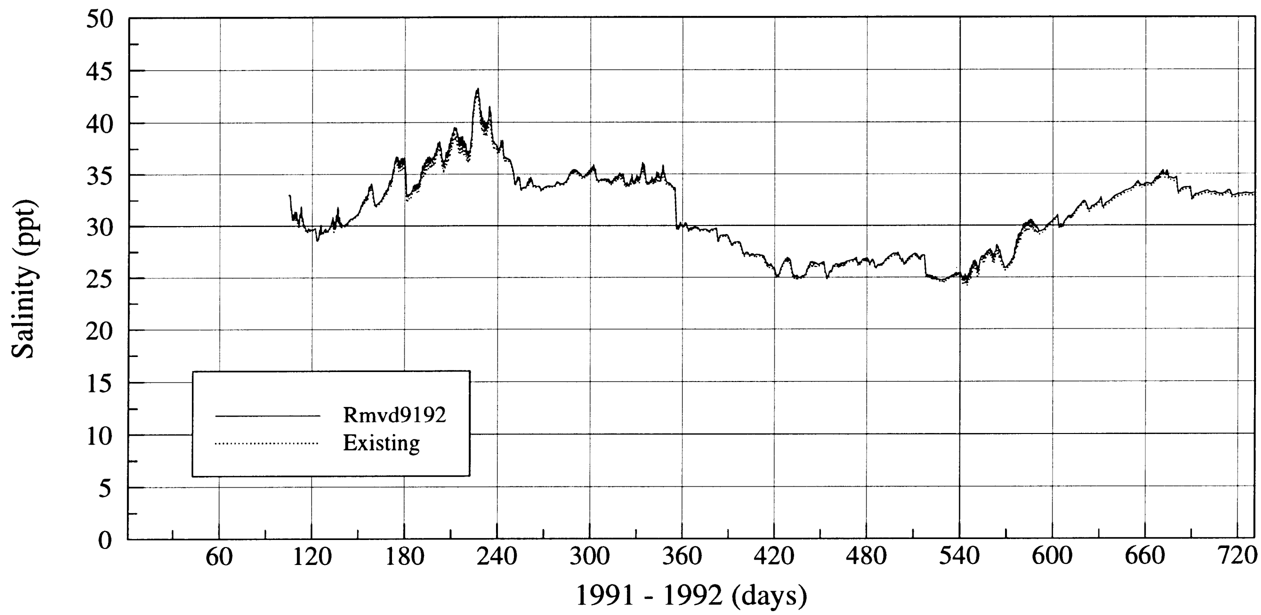

(d) Naval Air Station

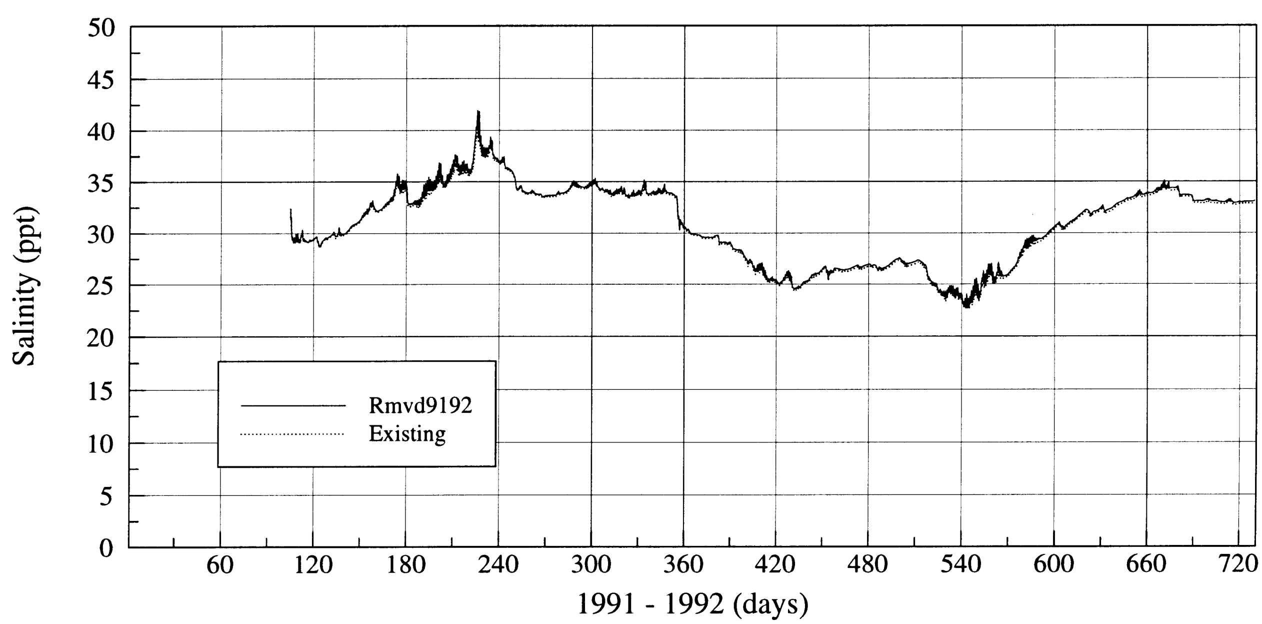

Figure IV.20 Simulated salinities in 1991-1992 for the existing condition and for the JFK Causeway removal scenario

(e) Baffin Bay

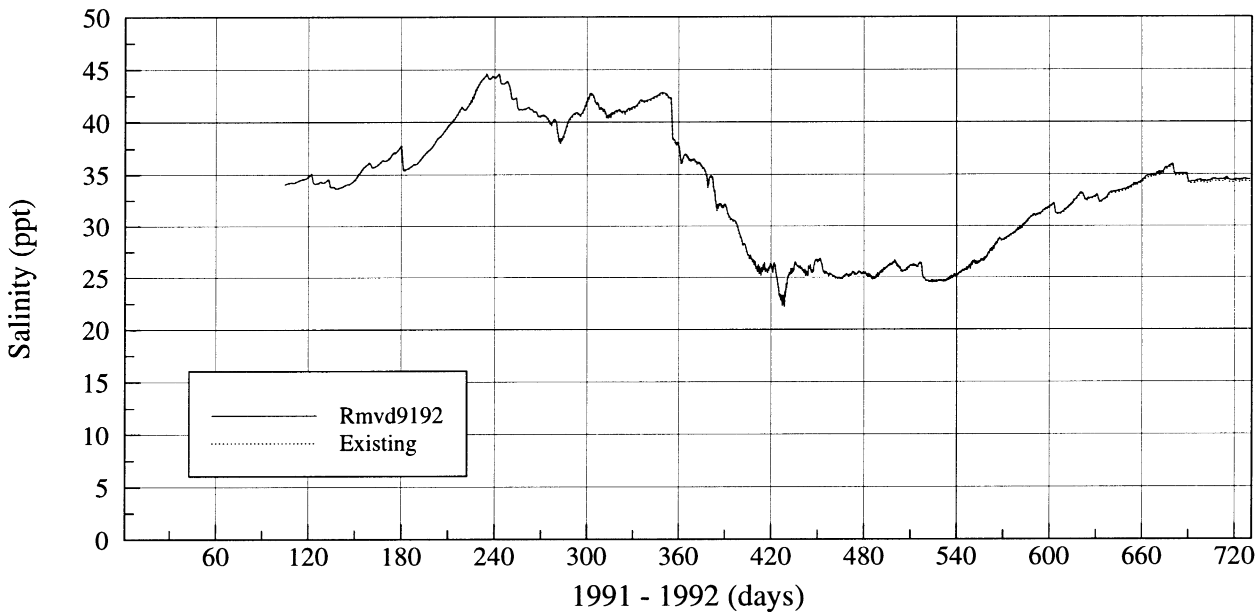

(f) GIWW near Pita Island

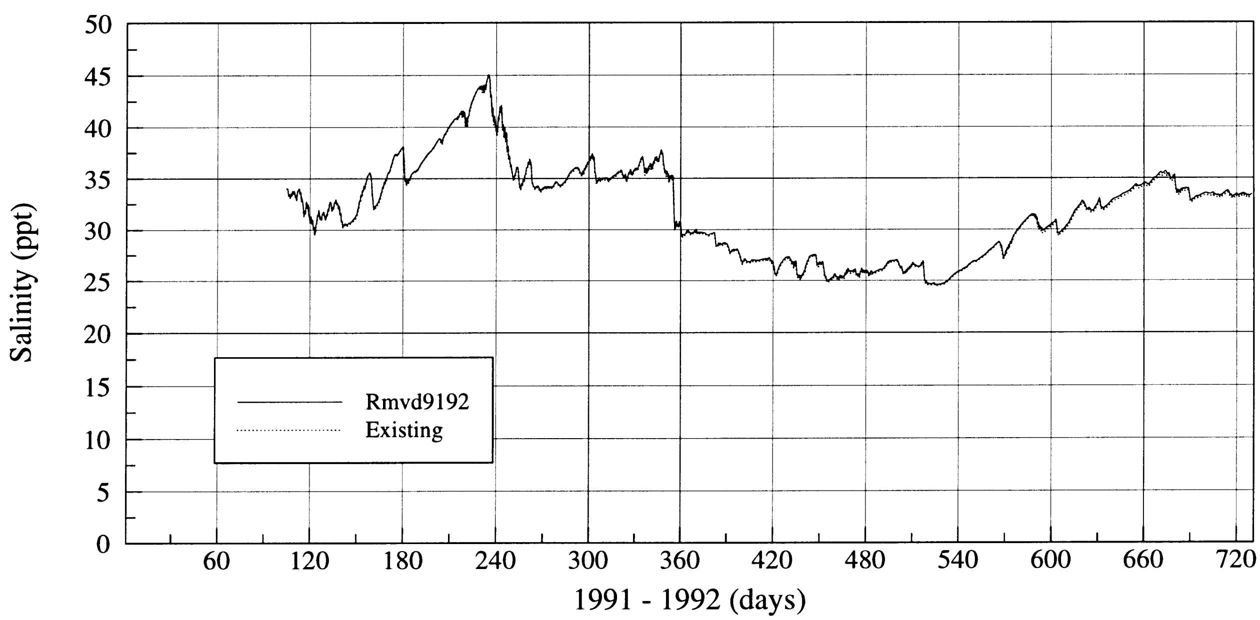

Figure IV.20 Simulated salinities in 1991-1992 for the existing condition and for the JFK Causeway removal scenario

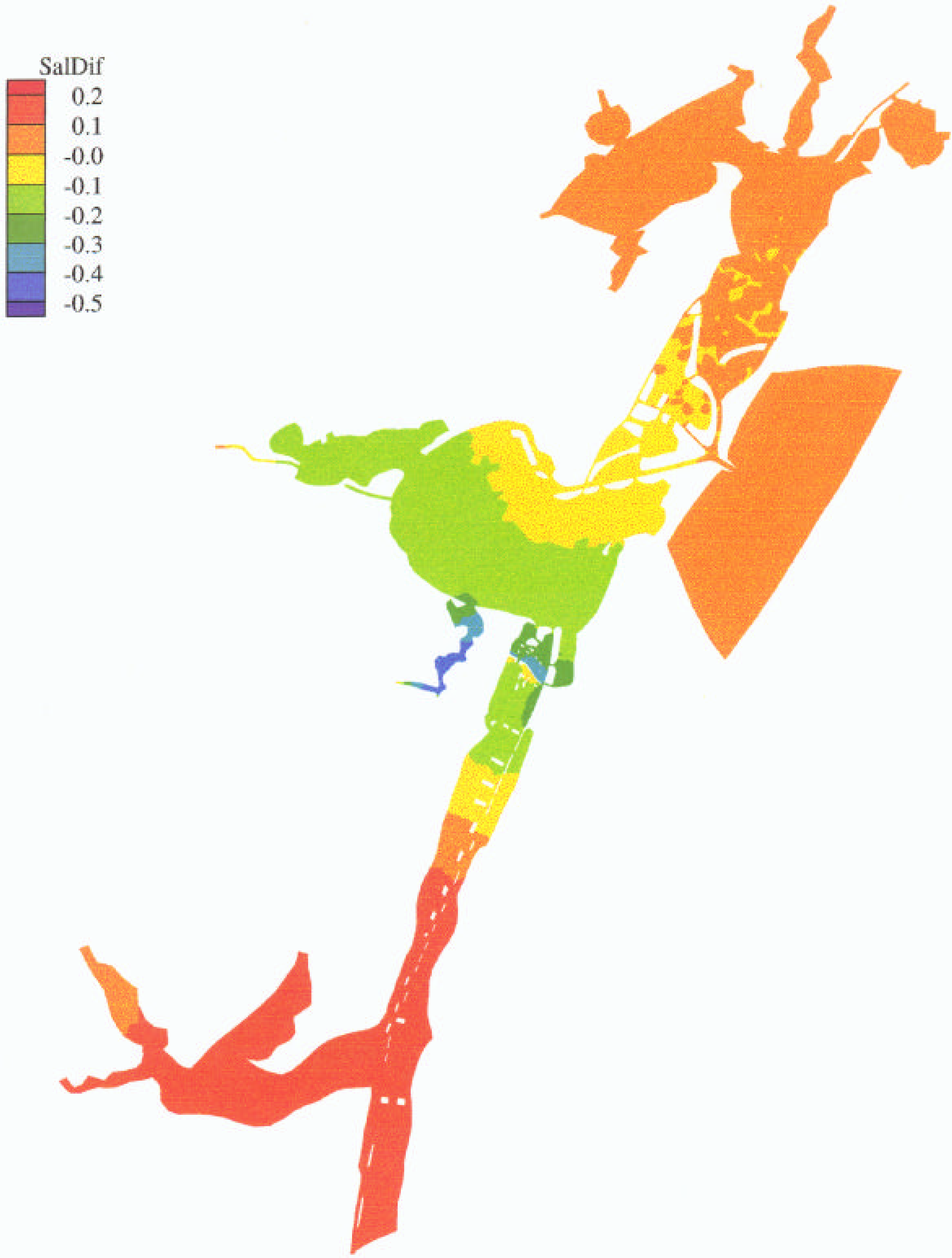

Figure IV.21 Salinity differences (ppt) in August 1989 between the existing and the JFK Causeway removal cases

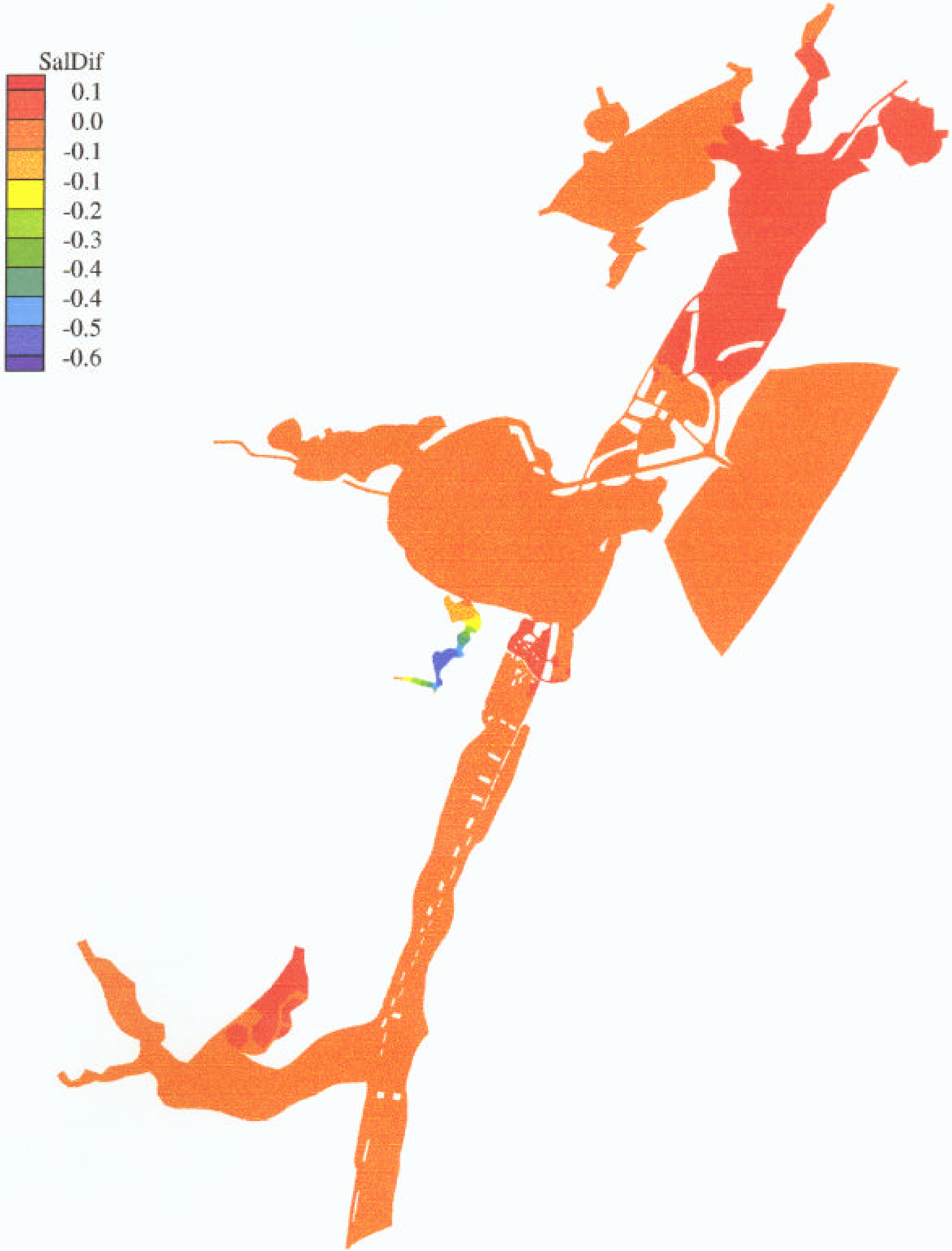

Figure IV.22 Salinity differences (ppt) in May 1992 between the existing and JFK Causeway removal cases

(a) Inflows and outflows for 1988-1989 existing and JFK Causeway removal cases

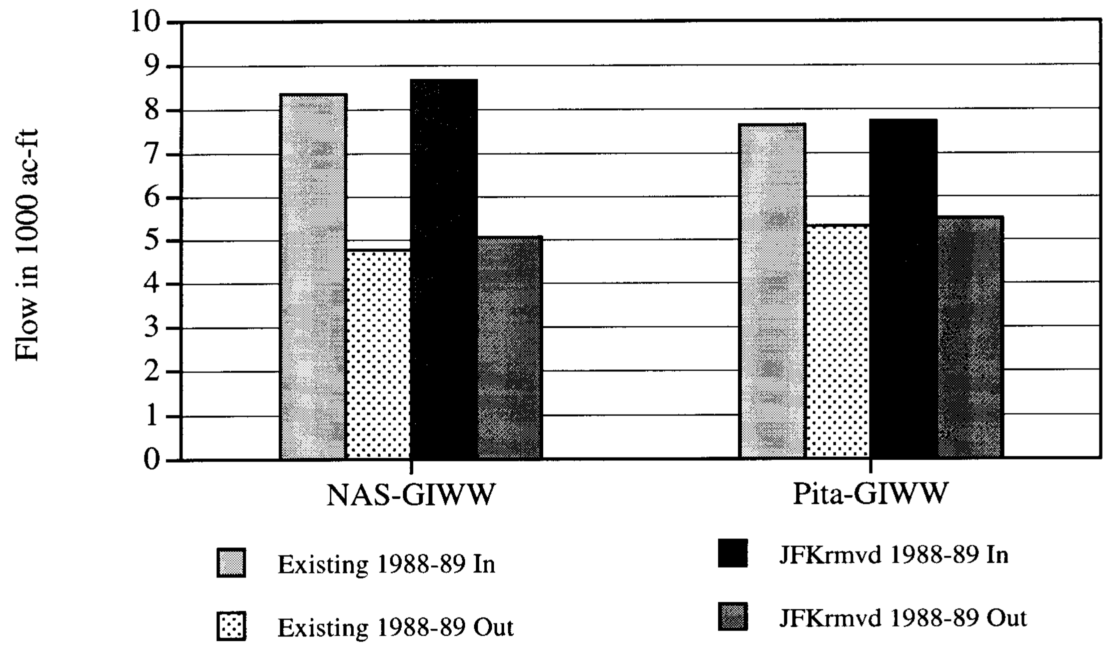

(b) Inflows and outflows for 1991-1992 existing and JFK Causeway removal cases

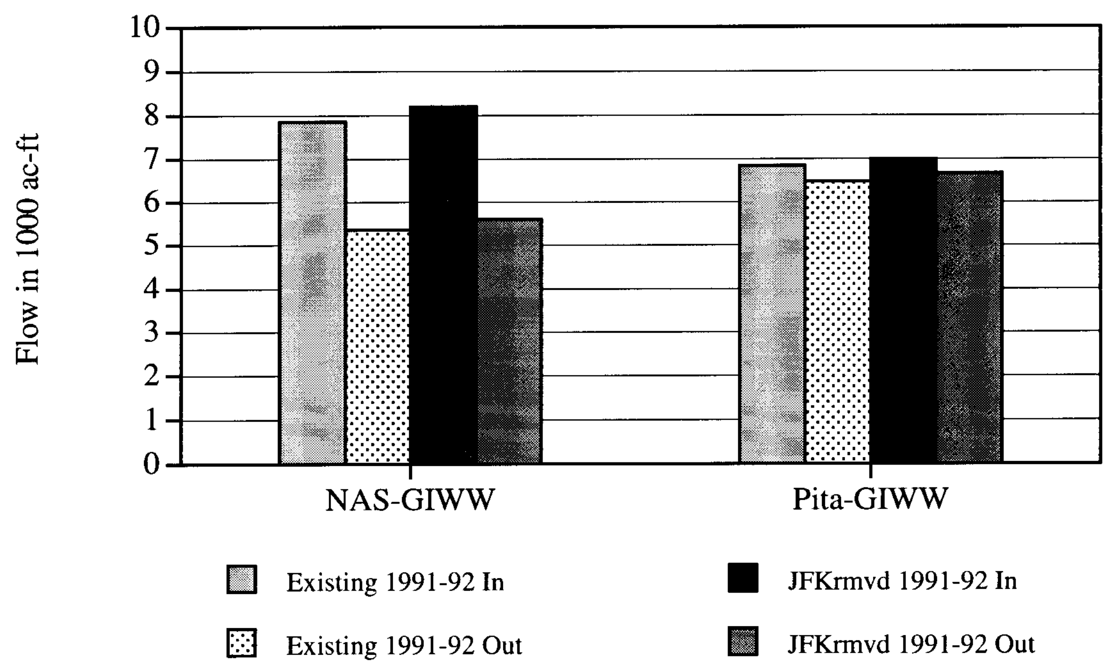

Figure IV.23 Average daily inflows and outflows at JFK Causeway area for the 1988-1989 and 1991-1992 existing condition and JFK Causeway removal cases

Scenario 4: Effect of Corpus Christi Ship Channel

The purpose of Scenario 4 is to examine the effect of Corpus Christi Ship Channel. The effect was studied by removing the channel from the model and changing the bathymetries of the channel (45 feet) to depths similar to the surrounding areas, mostly 10 to 12 feet.

Table IV.11 lists the monthly average salinity differences between the existing and the channel removal case for the 1988-1989 and 1991-1992 simulations. Figures IV.24(a) through IV.24(f) for 1988-1989 and Figures IV.25(a) through IV.25(f) for 1991-1992 are the time histories of scenario salinities at selected locations compared with the existing condition. Figure IV.26 is a plot of salinity differences for August 1989 and Figure IV.27 for May 1992.

The long-term salinity simulations for the 1988-1989 dry period in Figure IV.24 shows that salinities in Nueces and Corpus Christi bays, at the JFK Causeway, and near the Naval Air Station and Pita Island would be elevated 1 to 2‰ by removal of the channel. During the dry period, salinity levels would decline slightly in Aransas Bay (Table IV.11). The situation is more complicated in Baffin Bay where a prolonged period of hypersaline conditions would have been reduced by as much as 1.5‰ with channel removal. Once salinities were in the 40 to 45‰ range, however, channel removal would raise salinities by as much as 2‰.

During the 1991-1992 wet period, salinities would generally be slightly lower in all the bays with removal of the ship channel due to reduced tidal exchange between the Gulf and bays. The greatest effects of ship channel removal were seen in Corpus Christi and Aransas bays where salinities in some months were more than 3‰ lower. The effect of the channel is noticeable as far away as Baffin Bay where salinities would be as much as 2‰ lower without the channel. The effect of Corpus Christi Ship Channel generally is to reduce the magnitude and duration of high salinity periods as well as low salinity periods. Without the ship channel, the salinity during 1989 dry period would be 1 to 3‰ higher in bays other than Baffin and Aransas bays; during the 1992 wet period, the salinity would be lower by more than 3‰.

Tables IV.12 and IV.13 compare the flows at selected cross-sections with the existing condition and 'no ship channel' case, and Figure IV.28 compares them graphically. Removal of the Corpus Christi Ship Channel greatly reduces flow exchange to one-fourth of the current level at the Entrance Channel, to one-sixth of the current level at the Corpus Christi Ship Channel near Brown & Root, to one-third of the current level at the Nueces Causeway, and to about half at Lydia Ann Channel. This is not nearly as much as the reduction of flows at the Corpus Christi Ship Channel near Brown & Root, a site about the same distance from the entrance to the Gulf as Lydia Ann Channel. The relatively deep bathymetry of Lydia Ann Channel is natural and was not changed for the no-channel case simulation. Lydia Ann Channel is naturally maintained by the strong tidal flows between the Gulf and Aransas Bay, freshwater flows from the Mission- Aransas and Guadalupe estuaries, and strong north or northwest winds during northers that push water out the Aransas Pass. At the Laguna Madre side, flows are reduced to two-thirds to half of the current level.

Table IV.11 Salinity differences between the existing condition and Corpus Christi Ship Channel removal. The difference is positive if the existing salinity is higher than the simulated salinity.

Year	Month	Aransas Bay	Nueces Bay	Corpus Bay	Naval Air Sta.	GIWW JFK	GIWW Pita	Baffin Bay
1988	1	0.76	0.14	0.34	0.09	0.05	0.01	0.23
1988	2	2.12	0.44	0.76	0.53	0.43	0.31	0.24
1988	3	2.49	0.77	0.91	0.87	0.76	0.53	0.27
1988	4	1.89	0.76	0.63	0.83	0.86	0.82	0.30
1988	5	1.44	0.48	0.38	0.57	0.62	0.67	0.71
1988	6	0.98	0.21	0.20	0.27	0.31	0.39	1.11
1988	7	0.99	-0.08	-0.16	-0.06	0.03	0.23	1.42
1988	8	0.68	-0.38	-0.49	-0.46	-0.42	-0.26	1.63
1988	9	0.33	-0.57	-0.41	-0.59	-0.59	-0.59	0.43
1988	10	0.82	-0.43	-0.23	-0.39	-0.47	-0.61	0.09
1988	11	0.83	-0.30	-0.18	-0.27	-0.34	-0.55	0.05
1988	12	0.76	-0.30	-0.21	-0.23	-0.25	-0.28	0.08
1989	1	0.70	-0.27	-0.10	-0.17	-0.16	-0.16	0.32
1989	2	0.65	-0.13	0.15	0.06	0.05	0.05	0.84
1989	3	1.24	0.00	0.15	0.12	0.08	-0.01	0.96
1989	4	0.60	0.00	0.00	0.07	0.10	0.13	1.05
1989	5	0.58	-0.12	-0.15	0.03	0.12	0.14	1.25
1989	6	-0.19	-0.45	-0.80	-0.85	-0.76	0.25	1.46
1989	7	0.04	-0.93	-1.15	-1.47	-1.63	-1.19	1.55
1989	8	0.12	-1.38	-1.30	-1.71	-1.77	-2.87	1.42
1989	9	-0.03	-1.54	-1.04	-1.44	-1.52	-2.14	-2.21
1989	10	0.25	-1.31	-0.83	-1.00	-1.01	-1.15	-1.36
1989	11	0.35	-1.16	-0.82	-0.96	-0.98	-1.11	-1.23
1989	12	0.85	-0.97	-0.75	-0.79	-0.83	-0.91	-0.86
1991	5	0.77	0.73	1.06	0.80	0.68	0.43	0.01
1991	6	0.85	1.41	1.42	1.22	0.93	0.33	0.03
1991	7	1.02	1.50	1.14	0.61	0.24	0.03	-0.03
1991	8	0.50	0.96	0.17	-0.13	-0.46	-0.54	-0.14
1991	9	0.22	0.08	-0.25	-0.32	-0.28	-0.54	-0.14
1991	10	0.58	-0.07	-0.06	-0.12	-0.15	-0.27	-0.02
1991	11	0.82	-0.21	-0.17	-0.04	-0.03	0.00	0.20
1991	12	1.43	-0.20	0.02	-0.14	-0.23	0.01	0.53
1992	1	1.92	0.39	0.63	0.29	0.17	0.12	0.91
1992	2	2.26	0.16	0.94	0.49	0.46	0.32	0.56
1992	3	3.13	1.07	1.51	0.99	0.76	0.42	0.82
1992	4	2.65	1.16	2.63	2.41	2.12	1.42	0.79
1992	5	3.49	1.37	3.30	2.98	2.57	1.55	1.25
1992	6	3.06	0.64	3.26	2.42	2.07	1.65	1.36
1992	7	2.77	2.40	2.44	1.74	1.53	1.46	1.38
1992	8	1.63	2.76	2.12	2.27	2.12	1.86	1.57
1992	9	1.04	2.38	1.77	2.25	2.26	1.98	1.63
1992	10	0.94	1.76	1.17	1.67	1.76	1.95	1.82
1992	11	1.11	1.35	0.92	1.19	1.24	1.48	1.96

Table IV.12 Average daily flows (1000 ac-ft) through cross-sections near the Entrance Channel and Nueces Causeway. In means flow from the Gulf, out means flow to the Gulf.

Scenario	Simulation Year	In/Out	Entrance Channel	Channel at Brown&Root	Lydia Ann Channel	Nueces Causeway
Existing	1988-1989	In	104.3	67.1	31.2	5.7
Existing	1988-1989	Out	104.2	64.9	33.1	6.1
NoCCChan	1988-1989	In	28.5	12.0	13.9	2.1
NoCCChan	1988-1989	Out	28.3	9.0	16.2	2.2
Existing	1991-1992	In	99.2	63.2	30.4	5.4
Existing	1991-1992	Out	103.7	64.1	33.3	6.7
NoCCChan	1991-1992	In	26.3	10.7	13.1	1.9
NoCCChan	1991-1992	Out	30.5	10.1	16.7	2.8

Table IV.13 Average daily flows (1000 ac-ft) through cross-sections near JFK Causeway. In means flow to the south, out means flow to the north.

Scenario	Simulation Year	In/Out	NAS-GIWW	Humble-JFK/GIWW	Pita-GIWW
Existing	1988-1989	In	8.36	9.30	7.63
Existing	1988-1989	Out	4.77	5.11	5.32
		Difference	3.59	4.19	2.31
NoCCChan	1988-1989	In	6.05	7.08	5.85
NoCCChan	1988-1989	Out	2.26	2.82	3.48
		Difference	3.79	4.26	2.37
Existing	1991-1992	In	7.86	8.72	6.84
Existing	1991-1992	Out	5.36	5.98	6.48
		Difference	2.50	2.74	0.36
NoCCChan	1991-1992	In	5.60	6.54	5.23
NoCCChan	1991-1992	Out	2.70	3.53	4.60
		Difference	2.90	3.01	0.63

Figure IV.26 shows the difference in salinity distribution between the existing condition and the scenario for August 1989, a period of high salinities. The purple and blue areas in the legend represent regions of the estuary complex for August 1989 where salinities would be lower than under the existing condition if the Corpus Christi Ship Channel were removed. Notice that most of Copano and Aransas bays would be of slightly lower salinity under this scenario, and Baffin Bay and the southern portion of the Laguna Madre south of Baffin Bay would also have lower salinity conditions under the scenario, although in the latter case the boundary conditions used in the simulations may strongly influence the salinity levels that were calculated. The increase in salinity of Redfish Bay would be very slight, but all of the rest of the estuarine area would have more saline conditions without the channel than with it. The salinity difference runs in a north-south gradient, with the smallest increase in the northern part of Corpus Christi Bay, and the largest increase occurring in the upper Laguna Madre, south of Pita Island. The salinity difference returns to zero just north of Baffin Bay. While the magnitude of the salinity difference between the existing condition and channel removal scenario varies from about -3‰ to +2‰, the effect is evident over a wide area. This scenario results in modification of one of the main forces shaping the salinity patterns throughout the estuarine area, tidal flux. Thus, it is not surprising that the effect is extensive.

Figure IV.27 shows the spatial salinity differences in May 1992, a wet period. This figure indicates the entire system is affected extensively but Aransas Bay appears most affected; salinity would be lower by 2.5 to 4.5‰. Redfish Bay and Corpus Christi Bay are next most affected where salinity would be lower by about 3‰. Laguna Madre would be lower by 1 to 3‰; Nueces Bay 0.5 to 2.5‰.

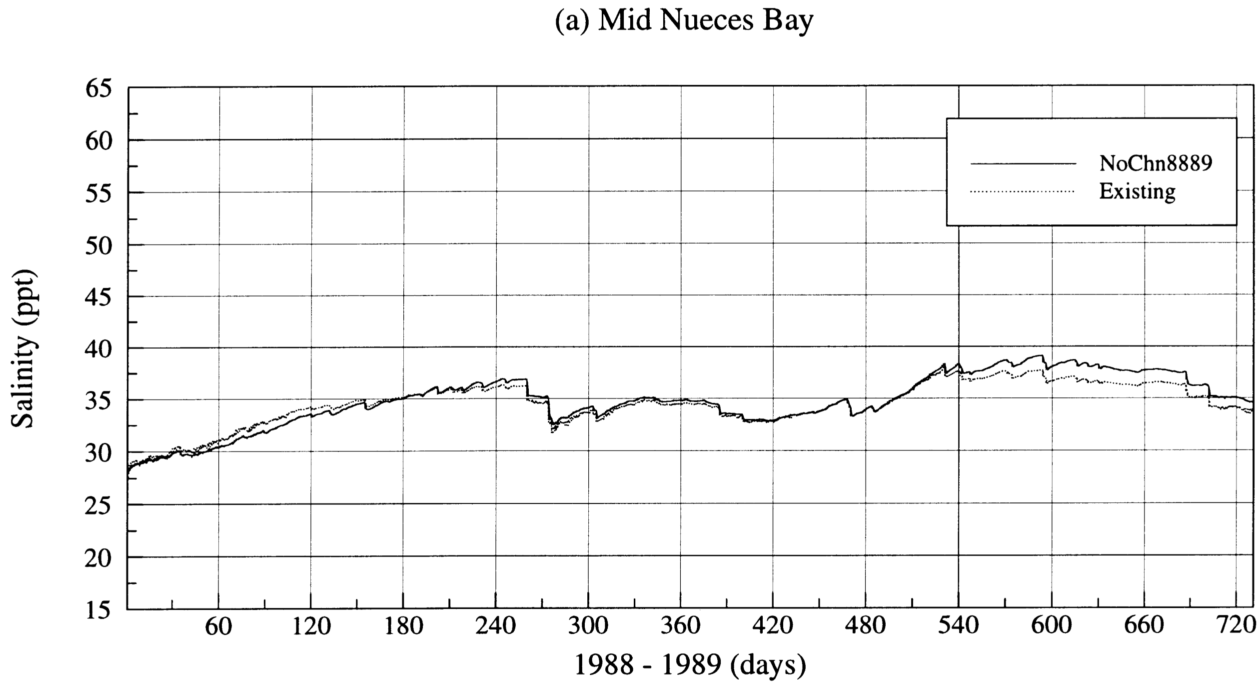

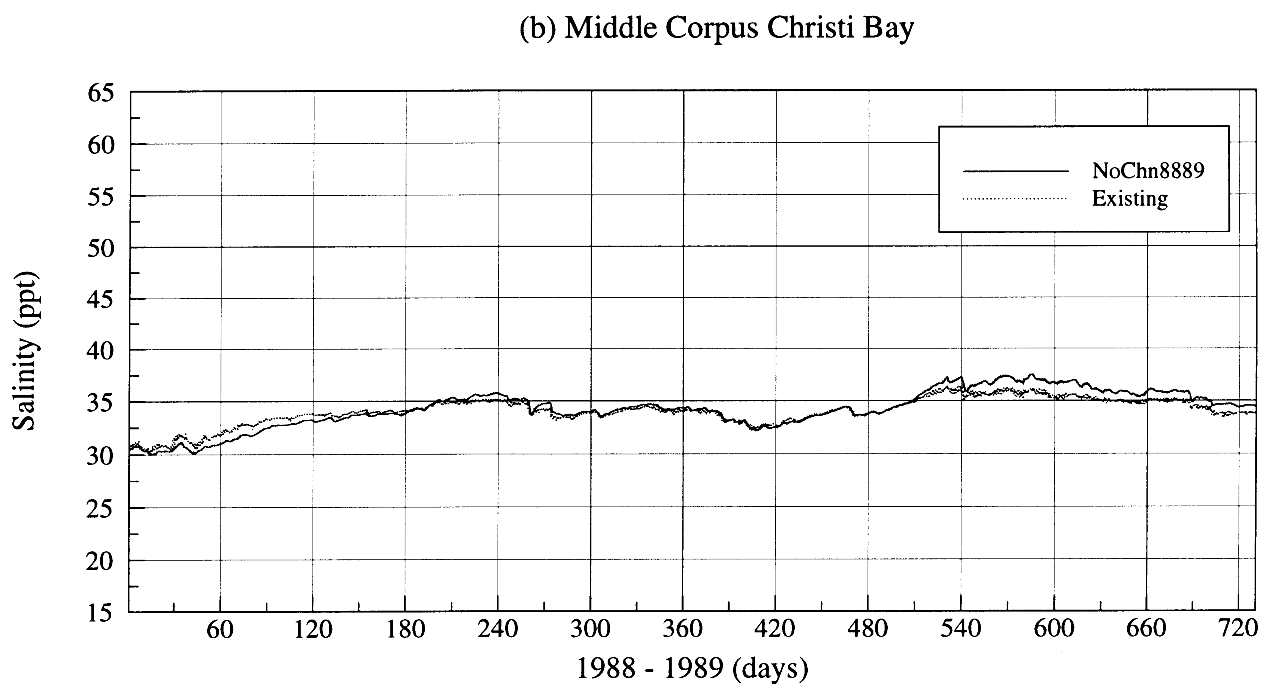

Figure IV.24 Simulated salinities in 1988-1989 for the existing condition and for the Corpus Christi Ship Channel removal scenario

(c) JFK Causeway

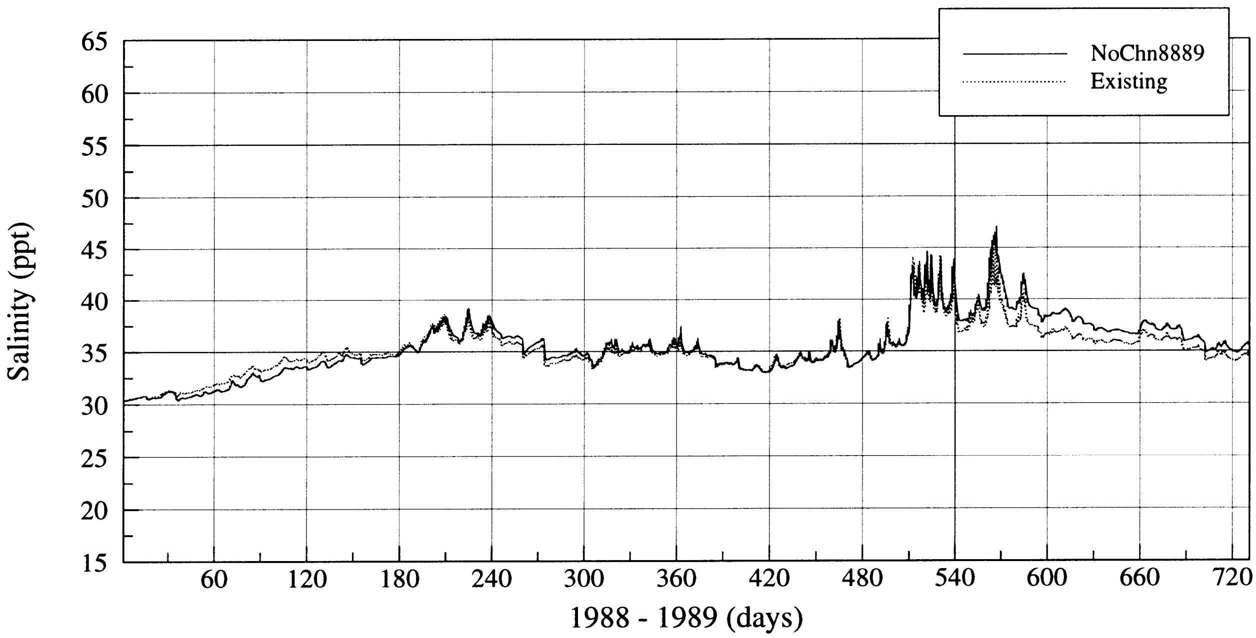

(d) Naval Air Station

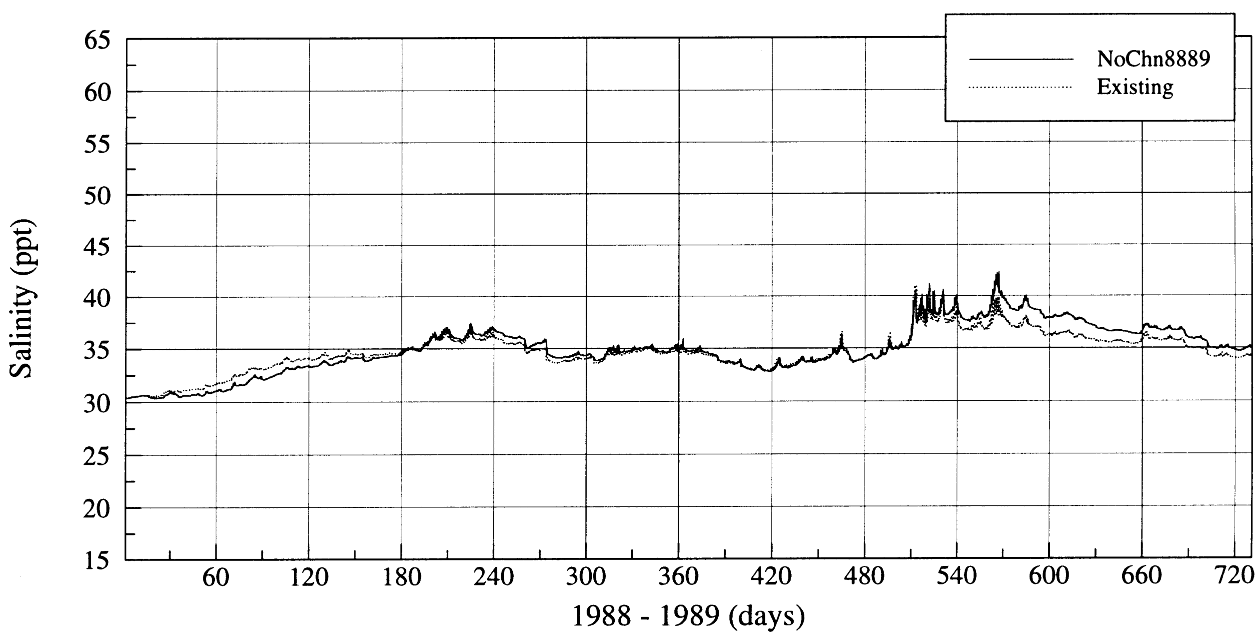

Figure IV.24 Simulated salinities in 1988-1989 for the existing condition and for the Corpus Christi Ship Channel removal scenario

(e) Baffin Bay

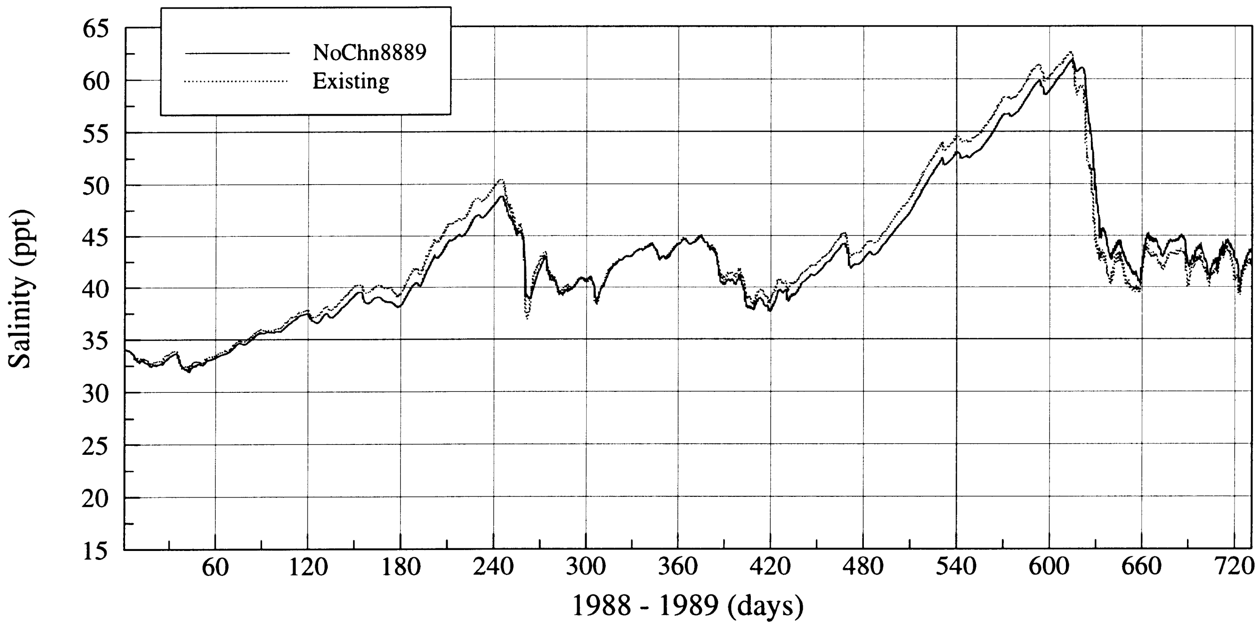

(f) GIWW near Pita Island

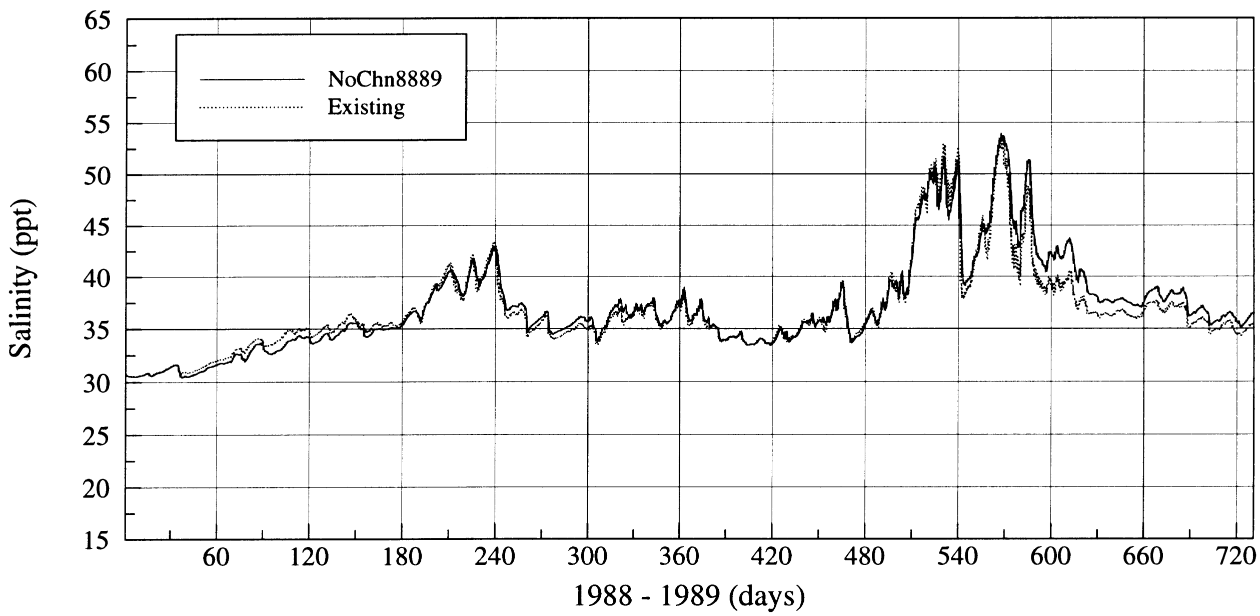

Figure IV.24 Simulated salinities in 1988-1989 the existing condition and for the Corpus Christi Ship Channel removal scenario

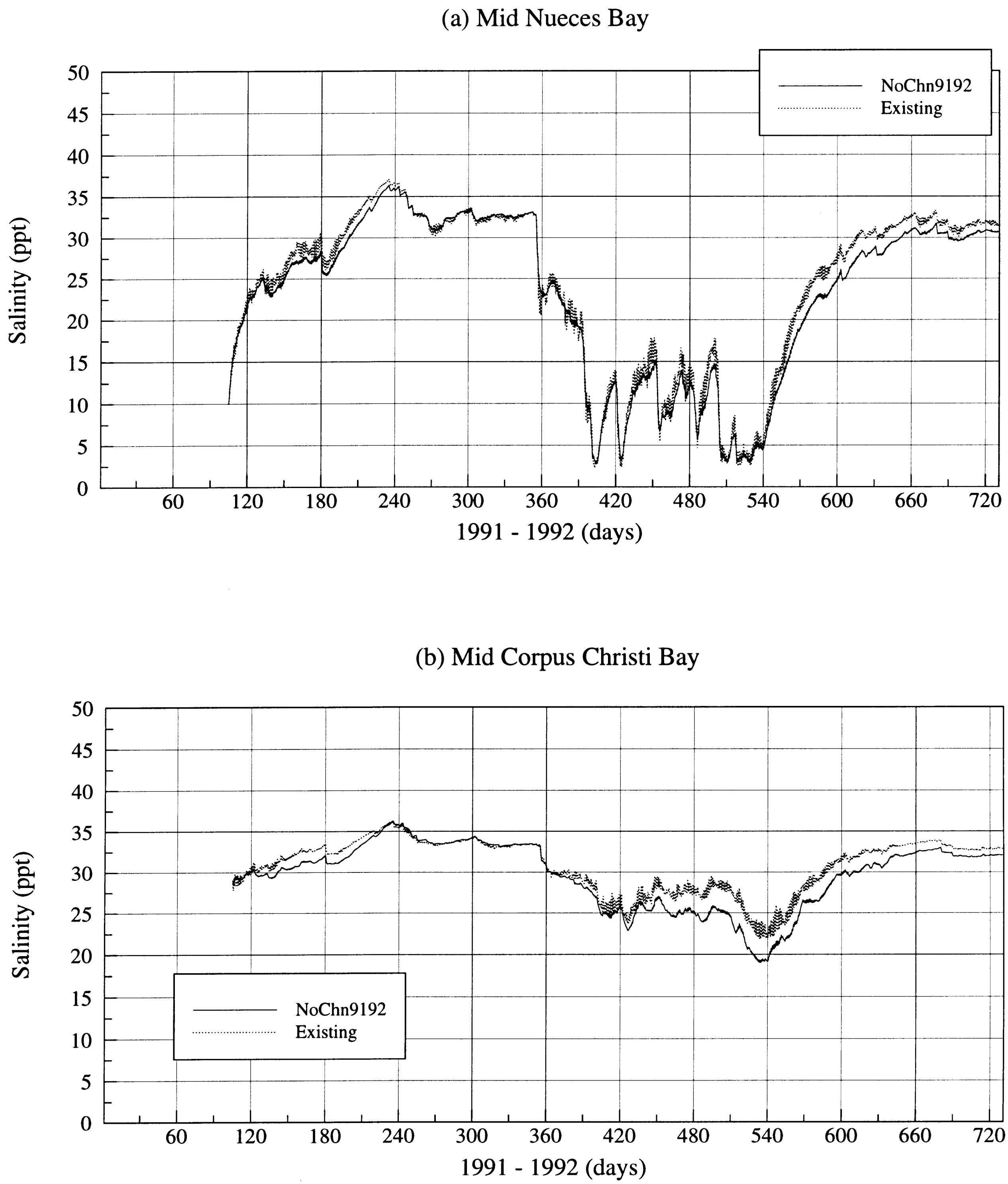

Figure IV.25 Simulated salinities in 1991-1992 for the existing condition and for the Corpus Christi Ship Channel removal scenario

(c) JFK Causeway

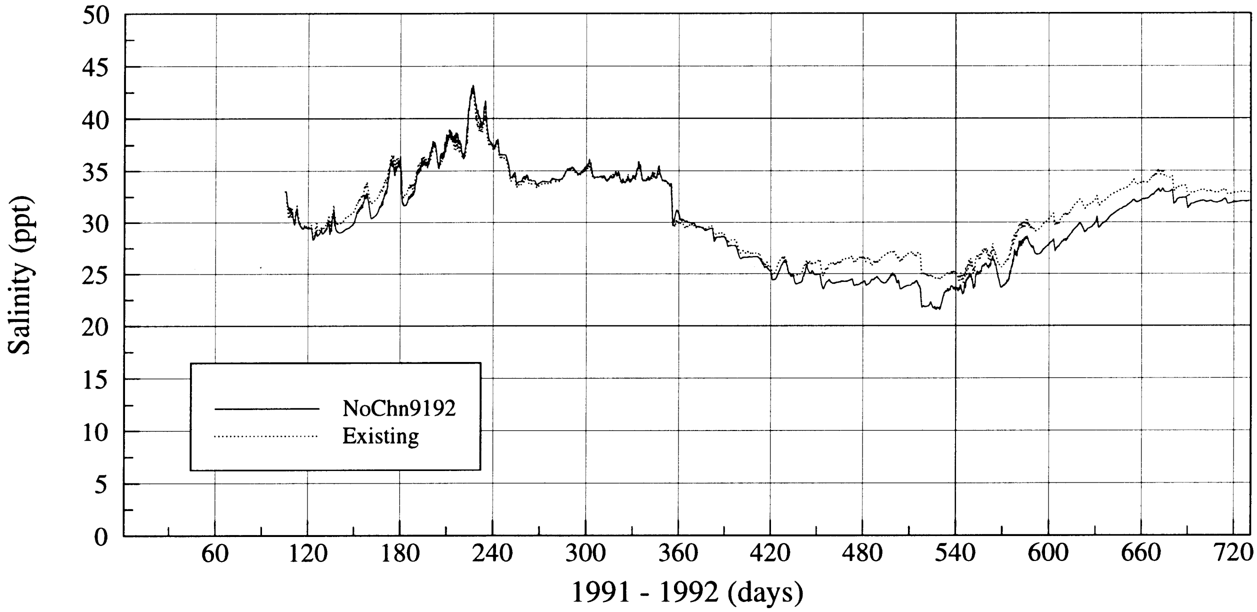

(d) Naval Air Station

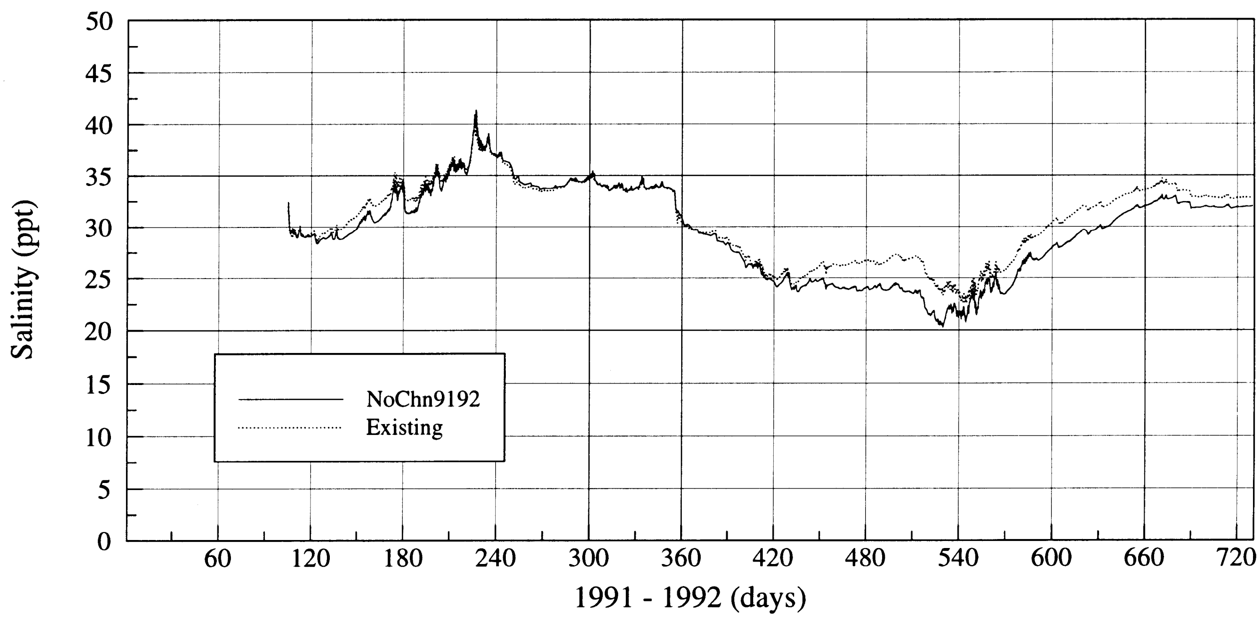

Figure IV.25 Simulated salinities in 1991-1992 for the existing condition and for the Corpus Christi Ship Channel removal scenario

(e) Baffin Bay

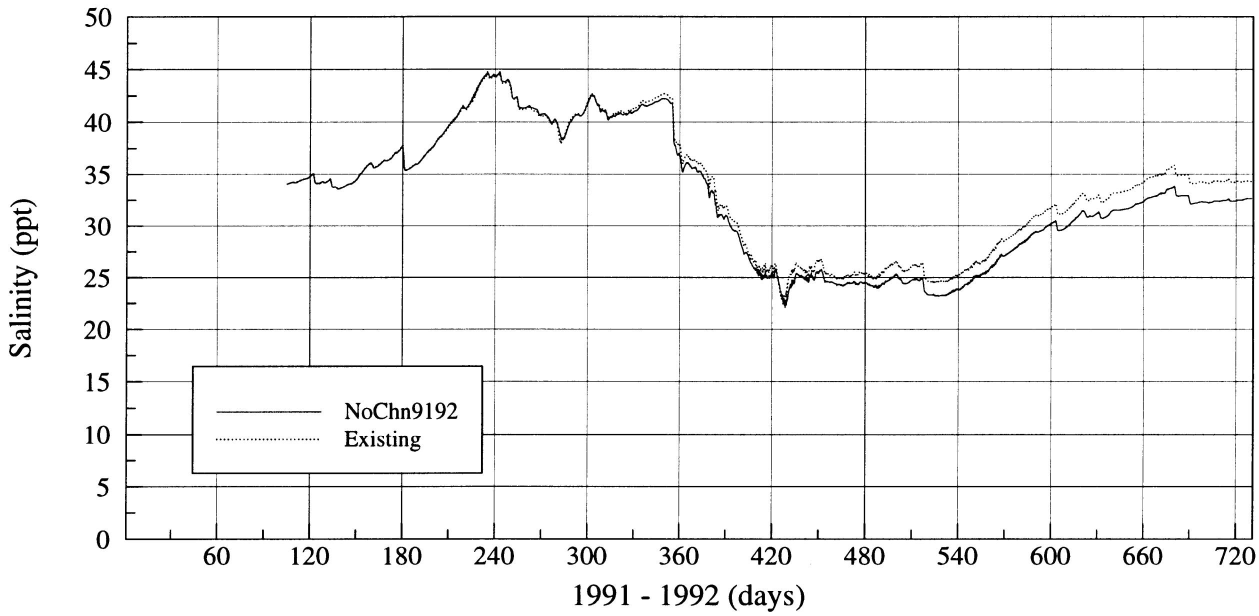

(f) GIWW near Pita Island

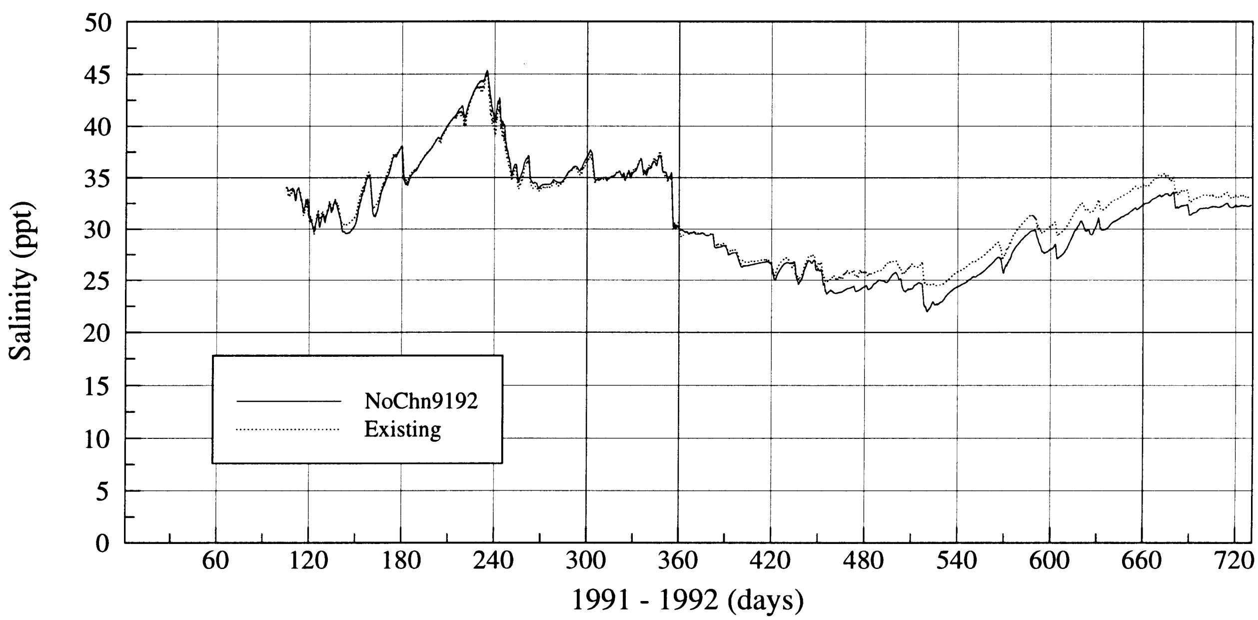

Figure IV.25 Simulated salinities in 1991-1992 for the existing condition and for the Corpus Christi Ship Channel removal scenario

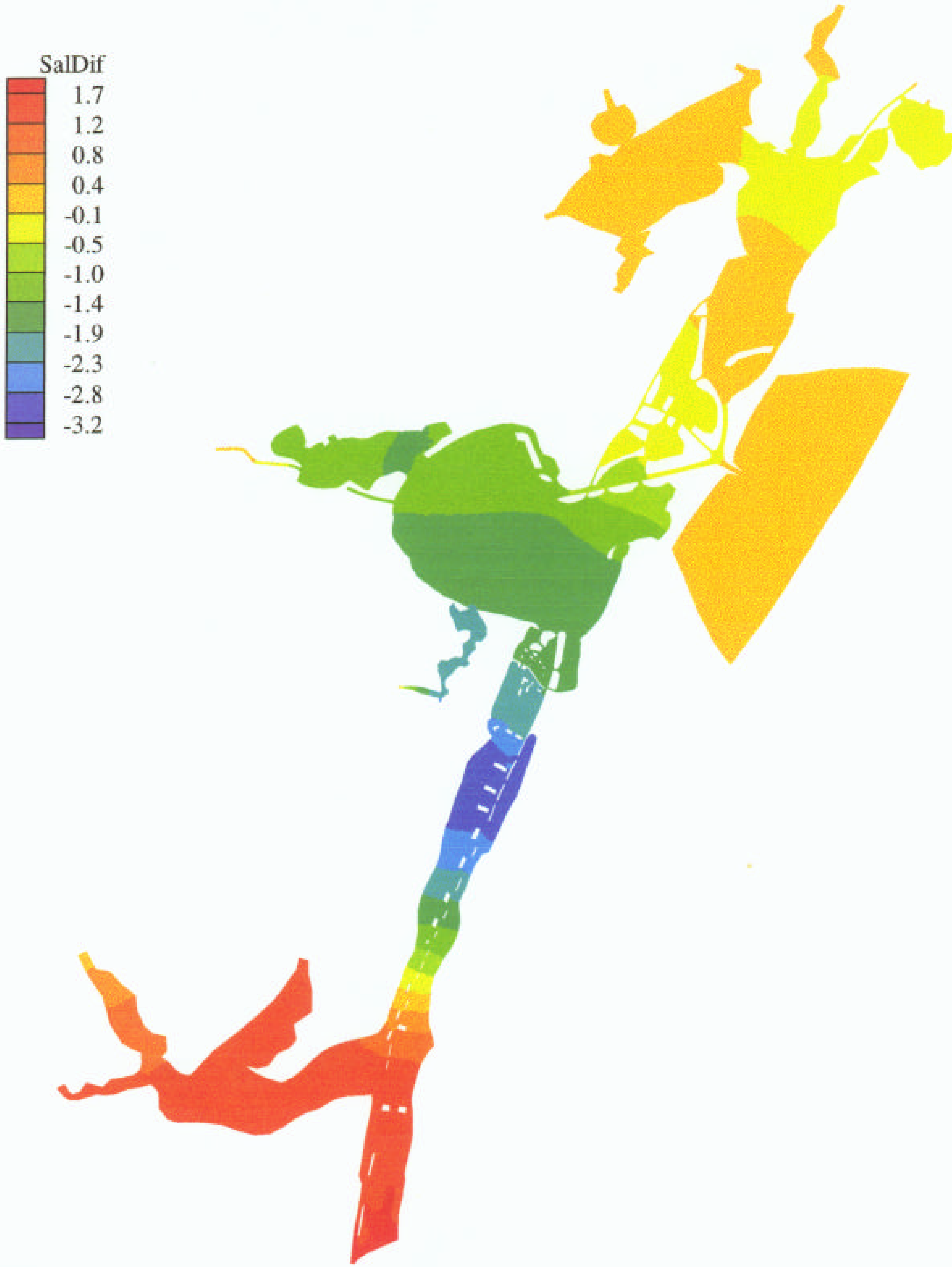

Figure IV.26 Salinity differences (ppt) in August 1989 between the existing and the Corpus Christi Ship Channel removal cases

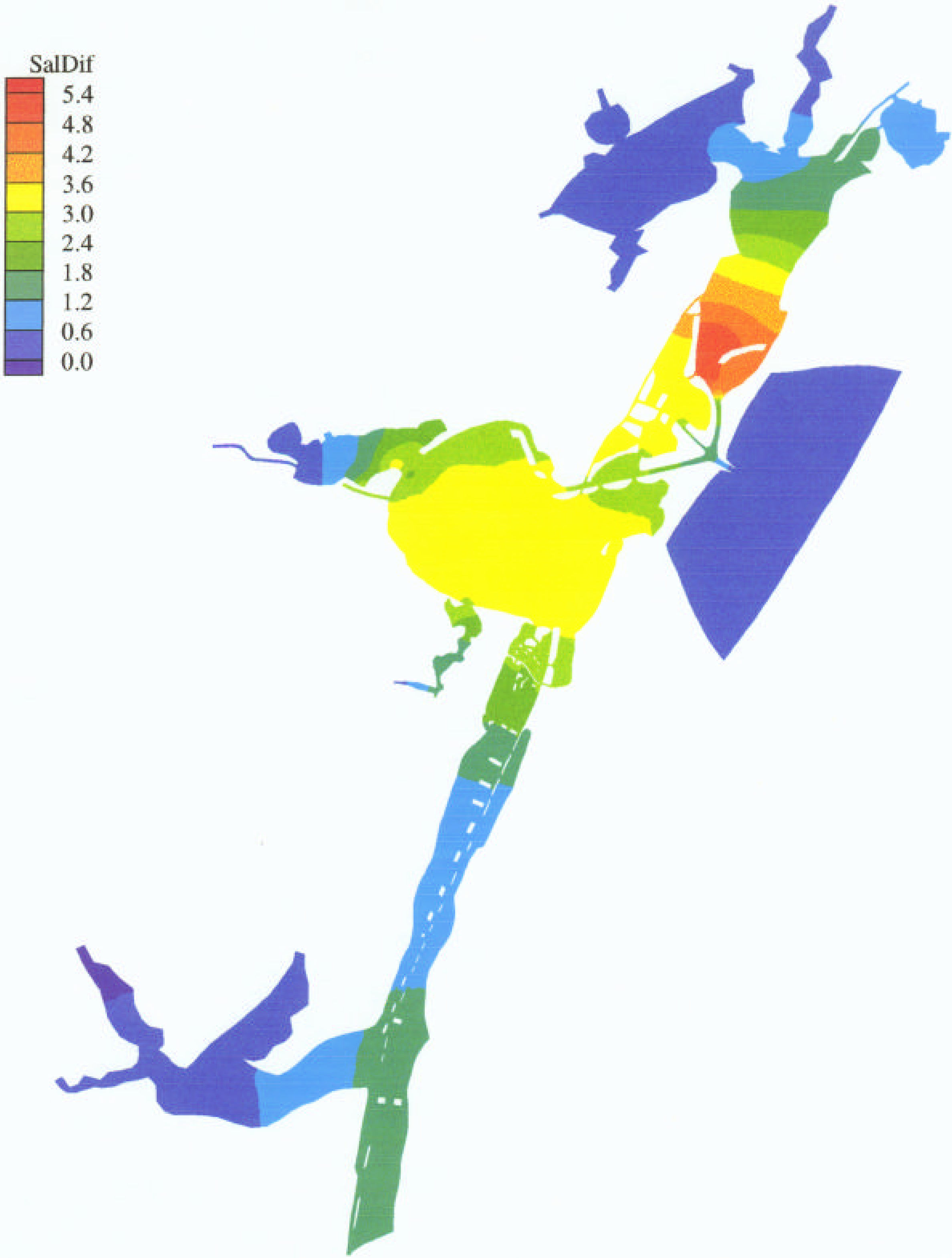

Figure IV.27 Salinity differences (ppt) in May 1992 between the existing and Corpus Christi Ship Channel removal cases

(a) Entrance Channel Area

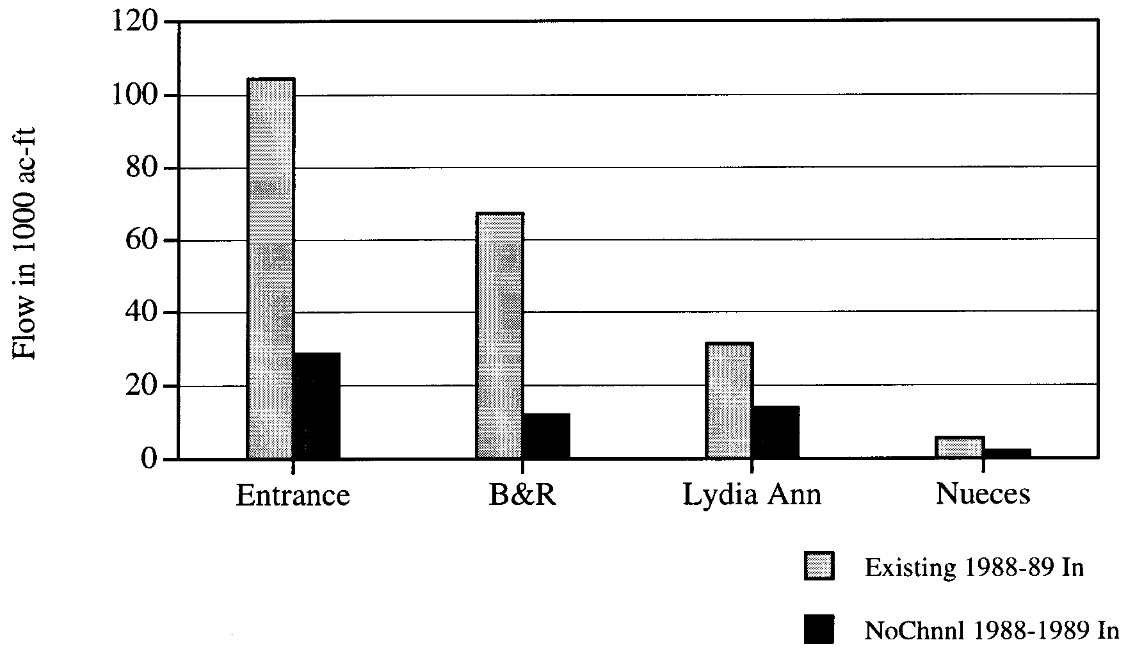

(b) JFK Causeway Area

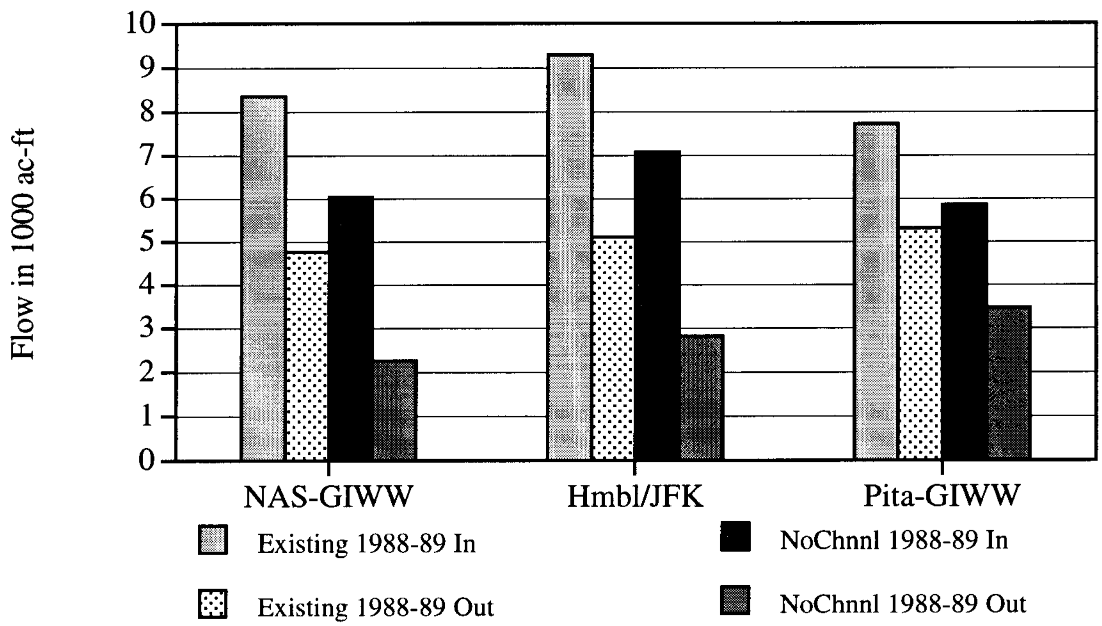

Figure IV.28 Average daily flows for the 1988-1989 existing condition and the Corpus Christi Ship Channel removal case

Scenario 5: All Impacts Removed

The purpose of Scenario 5 is to study the simultaneous effect of all structures and practices, including fresh water diversion, power plant operations, JFK Causeway, and Corpus Christi Channel. The effects were simulated by putting the diverted flow back into the Nueces River, by not taking seawater for cooling, by removing the JFK Causeway, and by removing the ship channel in the model.

Table IV.14 lists the differences in monthly average salinities between the existing and the all impacts case for the 1988-1989 and 1991-1992 simulations. Figures IV.29(a) through IV.29(f) for 1988-1989 and Figures IV.30(a) through IV.30(f) for 1991-1992 are the time histories of scenario salinities at selected locations compared with existing condition. Figure IV.31 is a plot of salinity differences for August 1989 and Figure IV.32 for May 1992.

The effect of all structure and practice impacts is strongest on Nueces Bay. The compound effects of increased inflow due to the return of diverted water to the Nueces River and the reduced tidal exchange through the Nueces Causeway due to the removal of Corpus Christi Channel cause the salinity differences. The salinity at the mid Nueces Bay site is lowered by 3 to 4‰ during 1989 dry period (Figure IV.29a), and 5 to more than 11‰ (Figure IV.30a) during the wet period of 1992.

Compound effects were also seen at the JFK Causeway site at the GIWW. The no-use of cooling water by power plant scenario by itself raised salinity by 2.4‰ during June and July of 1989. Coupled with the reduction in tidal exchange of this scenario, salinity increased by 2.5 to 3.4‰ during the same period (Figure IV.29(c)). Note that increased salinities occurred when salinity levels were above normal marine amounts (35‰); when salinities were below normal marine levels, the 'all impacts removed' scenario had salinities slightly below the existing salinities. During the May 1992 wet period, the 'all impacts removed' scenario lowered the salinity by as much as 5.0‰ which is greater than the combination of the no-cooling water case (lower by 1.7‰) and the no-ship channel case (lower by 2.6‰) taken together. The Naval Air Station and Pita Island stations showed the same patterns of elevated and decreased salinity as the JFK Causeway site.

For the Corpus Christi Bay calculation node, scenario salinities are slightly higher than existing salinities when salinity conditions are above normal marine levels (Figure IV.29(b)), and slightly below existing salinities when conditions are lower than normal marine salinities (Figure IV.30(b)). This is the result of reduced tidal exchange with channel removal. During the August 1989 dry period, the effects of the scenario raised salinity by 0.8‰, while during the 1992 wet period it lowered the salinity by as much as 6.3‰.

Table IV.14 Salinity differences between the existing condition and the all impacts removed case. The difference is positive if the existing salinity is higher than the simulated salinity.

Year	Month	Aransas Bay	Nueces Bay	Corpus Bay	Naval Air Sta.	GIWW JFK	GIWW Pita	Baffin Bay
1988	1	0.73	1.51	0.25	-0.01	-0.02	-0.01	0.35
1988	2	2.10	3.05	0.76	0.52	0.37	0.25	0.41
1988	3	2.50	3.69	1.13	0.97	0.74	0.51	0.54
1988	4	1.93	3.79	0.92	1.17	1.11	1.01	0.65
1988	5	1.45	3.30	0.63	0.87	0.84	0.95	1.19
1988	6	1.00	2.95	0.37	0.54	0.53	0.60	1.77
1988	7	1.01	2.88	0.00	-0.24	-0.31	0.48	2.36
1988	8	0.68	3.52	-0.29	-0.62	-1.09	-0.29	2.90
1988	9	0.34	2.63	-0.26	-0.38	-0.44	-0.44	1.22
1988	10	0.83	3.28	0.04	-0.04	-0.29	-0.40	0.70
1988	11	0.87	3.60	0.32	0.13	-0.17	-0.35	0.89
1988	12	0.79	3.97	0.35	0.26	0.04	0.06	1.21
1989	1	0.73	3.80	0.41	0.42	0.33	0.29	1.55
1989	2	0.67	3.91	0.60	0.58	0.54	0.60	1.87
1989	3	1.28	3.99	0.70	0.66	0.47	0.50	2.24
1989	4	0.67	3.73	0.57	0.56	0.43	0.63	2.63
1989	5	0.65	3.18	0.42	0.06	-0.07	0.96	3.00
1989	6	-0.12	2.96	-0.29	-1.49	-2.52	0.61	3.44
1989	7	0.06	3.98	-0.63	-2.20	-3.44	-1.41	3.63
1989	8	0.12	3.82	-0.85	-1.60	-2.48	-3.54	3.72
1989	9	-0.03	2.97	-0.71	-0.98	-1.29	-1.98	-0.24
1989	10	0.26	2.75	-0.55	-0.65	-0.76	-0.81	-0.59
1989	11	0.36	2.75	-0.49	-0.57	-0.69	-0.82	-0.35
1989	12	0.86	4.14	-0.21	-0.32	-0.47	-0.51	0.14
1991	5	0.04	6.22	1.31	0.59	0.17	0.00	-0.01
1991	6	0.56	8.17	2.11	0.87	0.31	0.19	0.05
1991	7	0.98	9.07	2.16	-0.18	-0.93	-0.05	-0.03
1991	8	0.63	8.26	1.20	-0.70	-2.05	-0.98	-0.19
1991	9	0.31	6.35	0.61	0.69	0.37	-0.46	-0.21
1991	10	0.66	5.91	0.80	0.83	0.68	0.69	0.45
1991	11	0.87	5.22	0.78	0.97	0.86	0.93	1.18
1991	12	1.51	5.32	1.05	1.02	0.74	0.97	1.71
1992	1	1.96	7.50	1.90	1.67	1.47	1.32	2.08
1992	2	2.34	5.07	3.00	2.37	2.03	1.69	1.31
1992	3	3.44	7.85	3.86	3.08	2.37	1.67	1.62
1992	4	2.84	8.12	5.06	5.00	4.60	3.60	1.62
1992	5	3.79	6.87	6.16	5.79	4.97	3.41	2.25
1992	6	3.37	4.08	6.28	4.45	3.77	3.26	2.38
1992	7	3.54	10.38	5.22	3.08	2.38	2.58	2.55
1992	8	2.36	11.76	4.59	4.46	3.91	3.50	2.86
1992	9	1.61	10.56	4.01	4.85	4.63	3.88	3.01
1992	10	1.41	8.84	2.92	3.92	4.11	4.47	3.62
1992	11	1.50	7.96	2.57	3.19	3.31	3.69	4.03

The effect of the 'all impacts removed' scenario on the Baffin Bay calculation node is to generally lower salinity. This occurred for most of the dry period simulations and the wet period simulations. For this node, the result of removing all impacts simultaneously appears to have a greater effect upon changing salinity than the sum of the individual effects of scenarios 1 through 4. However, the largest portion of the salinity decrease was due to Scenario 4, Corpus Christi Channel removal. The greatest salinity decrease was 4.0‰ during the 1991-1992 wet period.

The differences in salinity distribution for August 1989 in Figure IV.31 show that Nueces Bay is the area with greatest change from removal of all impacts; salinity in Nueces Bay would decrease from 0 to 10‰ in a gradient from the bay mouth to the river. Similar salinity differences are shown in Oso Bay. Baffin Bay and the Laguna Madre area south of Baffin Bay to the Land Cut would also have a salinity decrease of 3 to 4‰ in August 1989. Corpus Christi Bay would experience a small (0 to 1‰) salinity increase with removal of all impacts in August 1989. Upper Laguna Madre between Baffin Bay and the JFK Causeway would have the greatest increase in salinity, as much as 4‰. The effect of the removal of structures and practices on salinity of Aransas and Copano bays is essentially negligible.

Figure IV.32 depicts the salinity differences in May 1992 wet period for the 'all impacts removed' case. Nueces Bay and Oso Bay would be most affected due to no power plant operation and reduced tidal flow with removal of the Ship Channel. Corpus Christi Bay would also be significantly affected, as much as 7‰ lower in the upper bay near its western edge. The influence of the 'all impacts removed' case is gradually reduced to the north and the south with distance away from Corpus Christi Bay.

Tables IV.15 compares the flows around the Entrance Channel and Nueces Causeway for the 'all impacts removed' scenario with the existing case. These flows, greatly reduced by removal of the Ship Channel, are very similar to those in Table IV.12 for the channel removal scenario. Small differences are probably due to no power plant operation in the 'all impacts removed' scenario.

Table IV.16 compares the flows in Laguna Madre. They are similar to those in Table IV.13 in which the flows are reduced by ship channel removal. But there are dissimilarities too. The effect of JFK Causeway removal and no power plant operation complicates the comparison. For example, the flow into Laguna Madre at the NAS-GIWW is 4.70 thousand ac-ft for the 1991-1992 all impact scenario, the smallest volume among all scenarios. It is 5.60 thousand ac-ft for the ship channel removal scenario alone. But the Pita-GIWW flows are 5.71 thousand ac-ft for 'all impacts removed' and 5.23 thousand ac-ft for channel removal. Because there is no power plant operation in the 'all impacts removed' scenario, less flow comes from Corpus Christi Bay. But the flows to the south through Pita-GIWW section are increased because there is no causeway to block the flows.

Table IV.15 Average daily flows (1000 ac-ft) through cross-sections near the Entrance Channel and Nueces Causeway.

Scenario	SimuYear	In/Out	EnterChn	Chn-B&R	LydiaAnn	NueCswy
Existing	1988-1989	In	104.3	67.1	31.2	5.7
Existing	1988-1989	Out	104.2	64.9	33.1	6.1
AllImpct	1988-1989	In	27.2	11.0	13.7	2.4
AllImpct	1988-1989	Out	29.6	9.9	16.4	1.9
Existing	1991-1992	In	99.2	63.2	30.4	5.4
Existing	1991-1992	Out	103.7	64.1	33.3	6.7
AllImpct	1991-1992	In	25.2	9.8	12.9	2.2
AllImpct	1991-1992	Out	32.7	10.9	16.9	2.5

Table IV.16 Average daily flows (1000 ac-ft) through cross-sections near the JFK Causeway.

Scenario	SimuYear	In/Out	NAS-GIWW	Humble-JFK	Pita-GIWW
Existing	1988-1989	In	8.36	9.30	7.63
Existing	1988-1989	Out	4.77	5.11	5.32
		Difference	3.59	4.19	2.31
AllImpct	1988-1989	In	5.22	2.92[a]	6.35
AllImpct	1988-1989	Out	2.97	1.47[a]	3.49
		Difference	2.25	1.45[a]	2.98
Existing	1991-1992	In	7.86	8.72	6.84
Existing	1991-1992	Out	5.36	5.98	6.48
		Difference	2.50	2.74	0.36
AllImpct	1991-1992	In	4.70	2.75[a]	5.71
AllImpct	1991-1992	Out	3.63	1.50[a]	4.55
		Difference	1.07	1.25[a]	1.16

a) These flows do not include the flow through the removed portion of the causeway

Figures IV.33 and IV.34 are the plots of residual vectors for the ‘all impacts removed’ scenario. They were created with the same conditions as those for the existing condition. Compared to the existing case, these activities (or vectors) appear very small. (Vectors can be made larger by adjusting the plotting scale, but the scale was kept the same for a better comparison.) Yet they exhibit patterns worth noticing. In Figure IV.33, water comes to Nueces Bay through the deeper channel (Rincon Canal) and goes out of the bay through the shallow part of the channel under the Nueces Causeway. Then it moves along the northern shore of the bay. Along the southern shore of the bay, water moves toward Laguna Madre and enters through the pass near the Naval Air Station. But the water returns to the bay through the GIWW heading toward the middle of bay and recirculates near the south end of the Nueces Causeway.

Figure IV.34 shows the residual vectors in Laguna Madre and Oso Bay. Water flows south through the Humble Channel and the removed part of the JFK Causeway. It moves back to Corpus Christi Bay through the GIWW.

Figure IV.35 illustrates the flow traces for the ‘all impacts removed’ case. This figure should be compared with Figure IV.13 for the existing condition. It is clearly shown in Figure IV.35 that neither the removed ship channel nor the ceased power plant operations has influence on the net flow pattern.

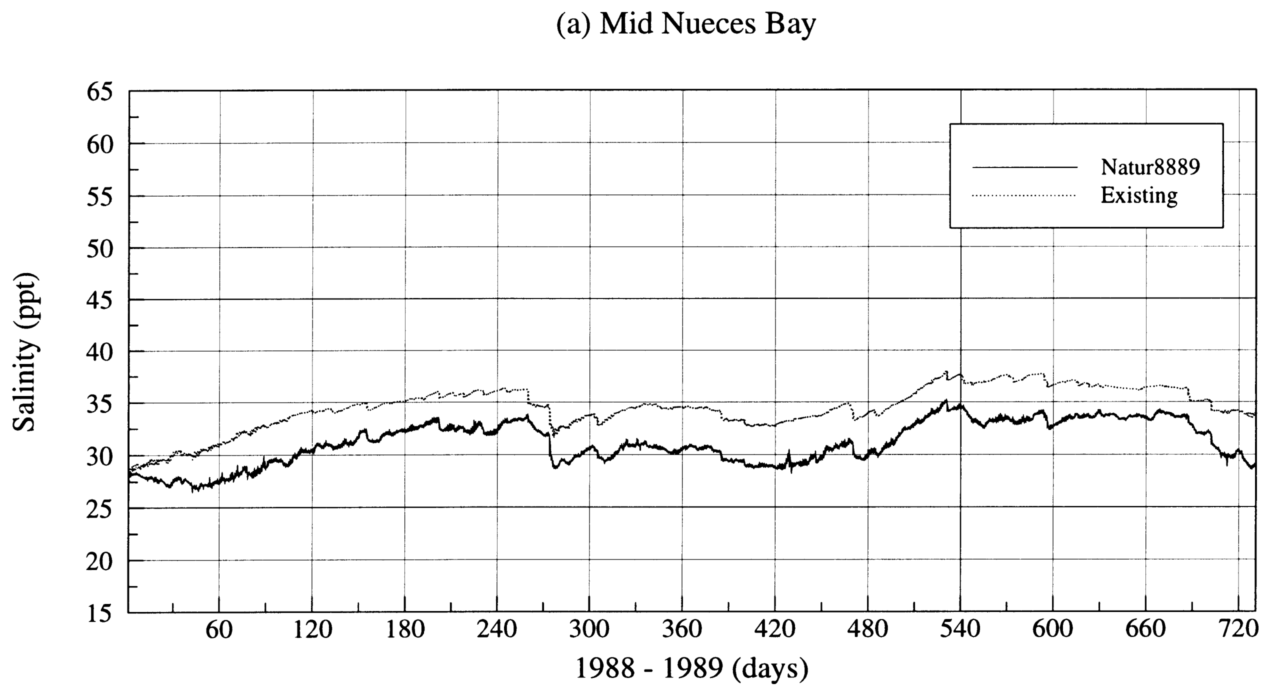

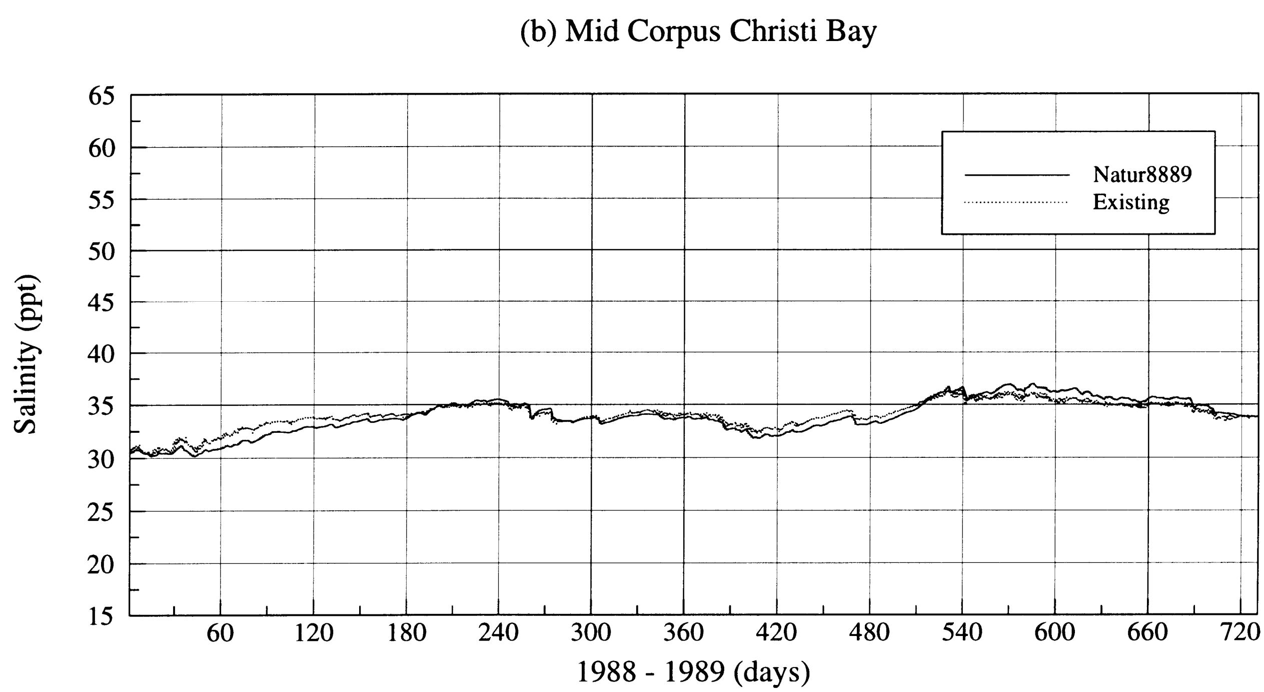

Figure IV.29 Simulated salinities in 1988-1989 for the existing condition and for the all impacts removed scenario

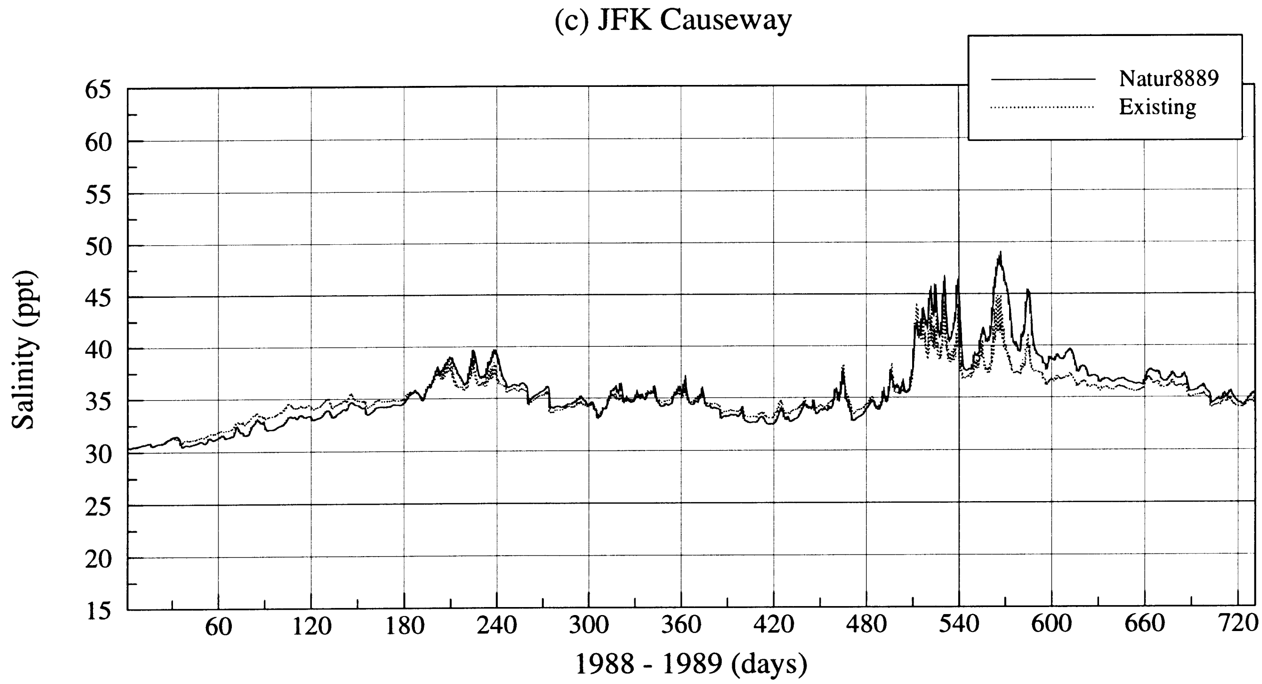

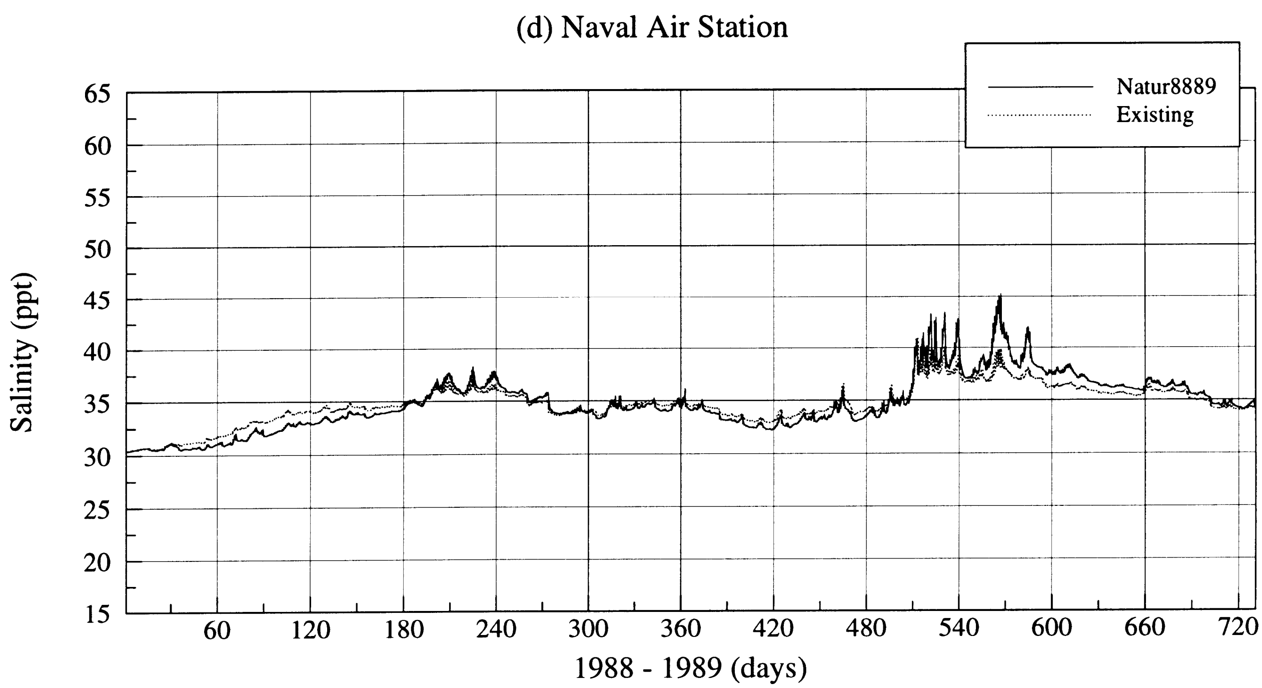

Figure IV.29 Simulated salinities in 1988-1989 for the existing condition and for the all impacts removed scenario

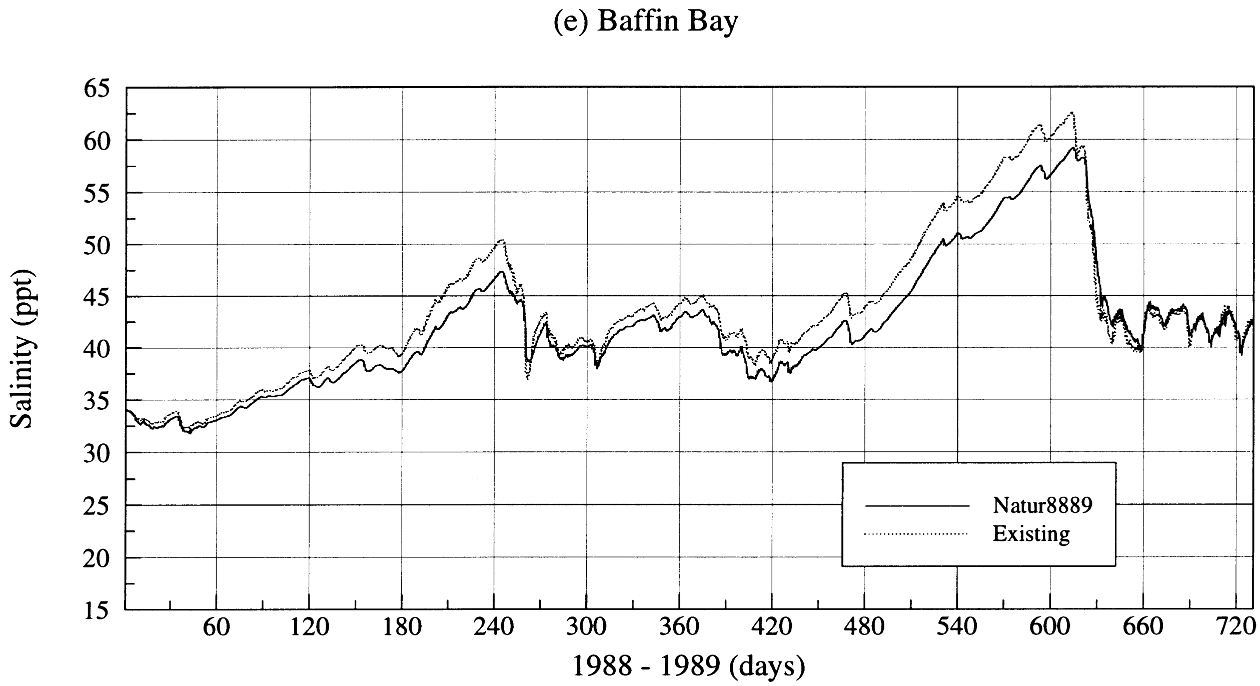

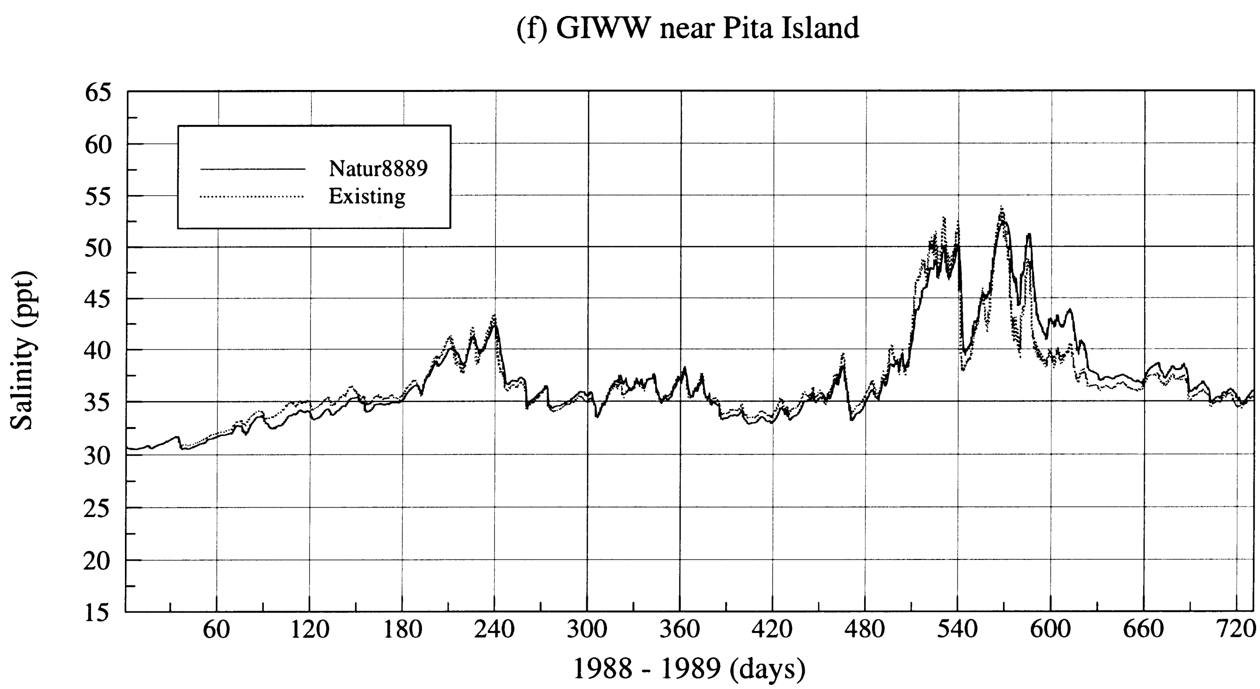

Figure IV.29 Simulated salinities in 1988-1989 for the existing condition and for the all impacts removed scenario

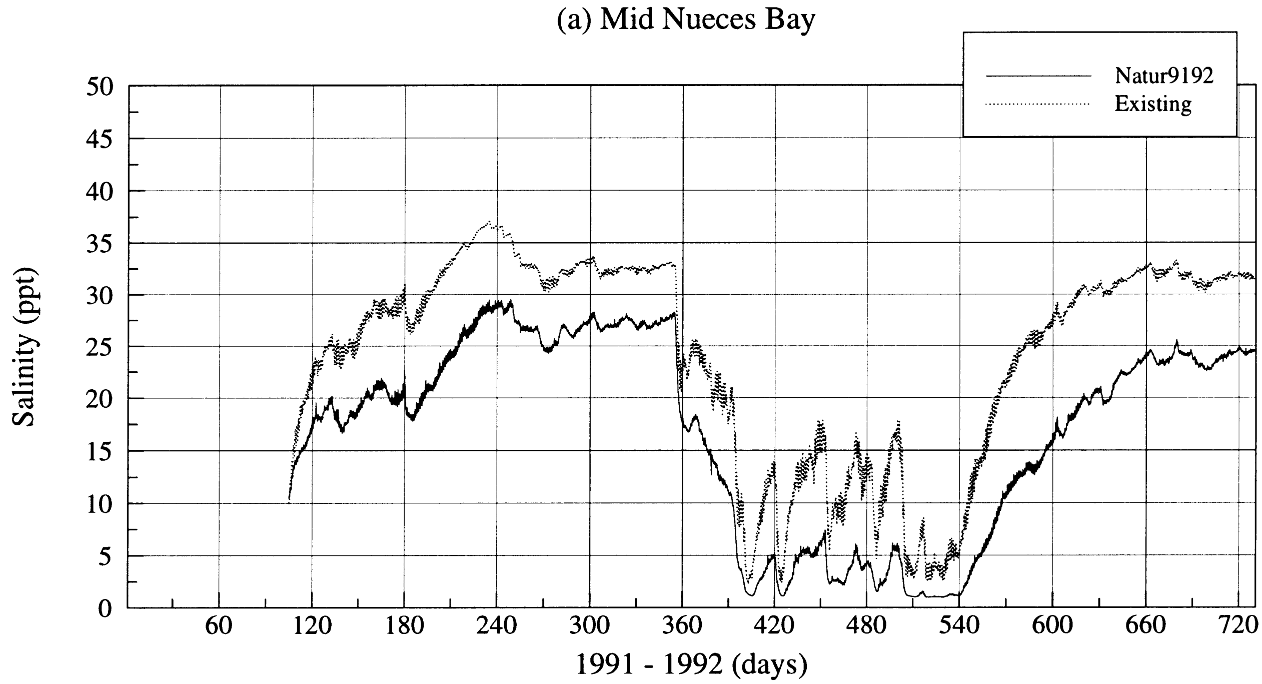

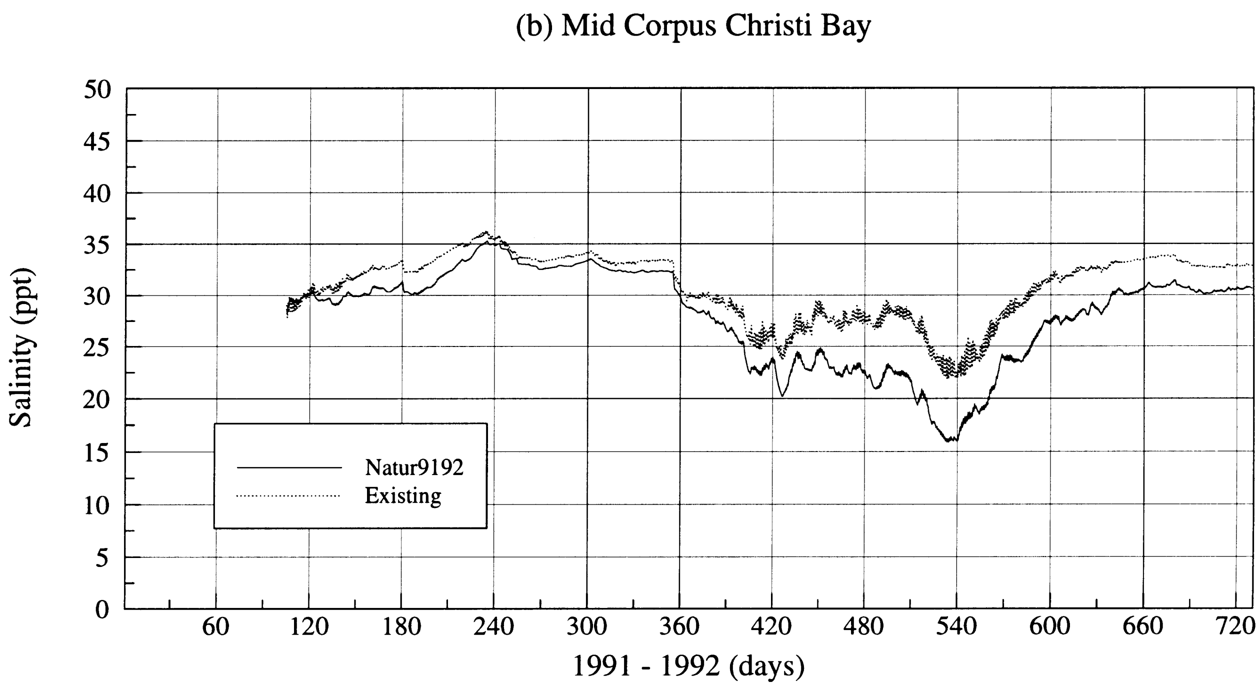

Figure IV.30 Simulated salinities in 1991-1992 for the existing condition and for the all impacts removed scenario

(c) JFK Causeway

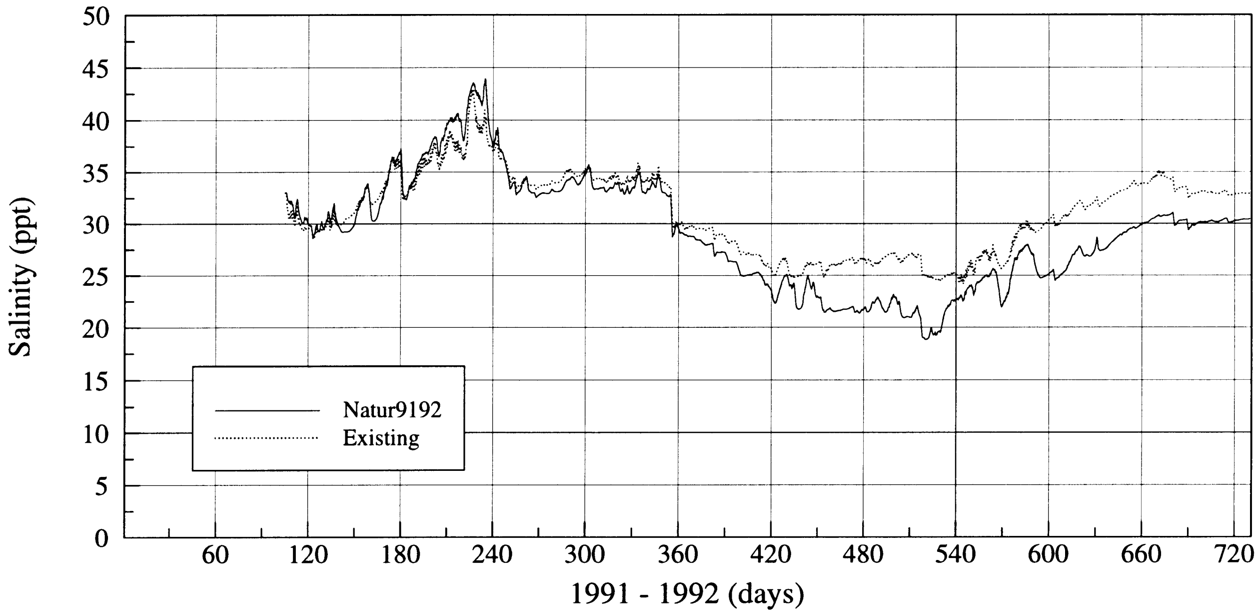

(d) Naval Air Station

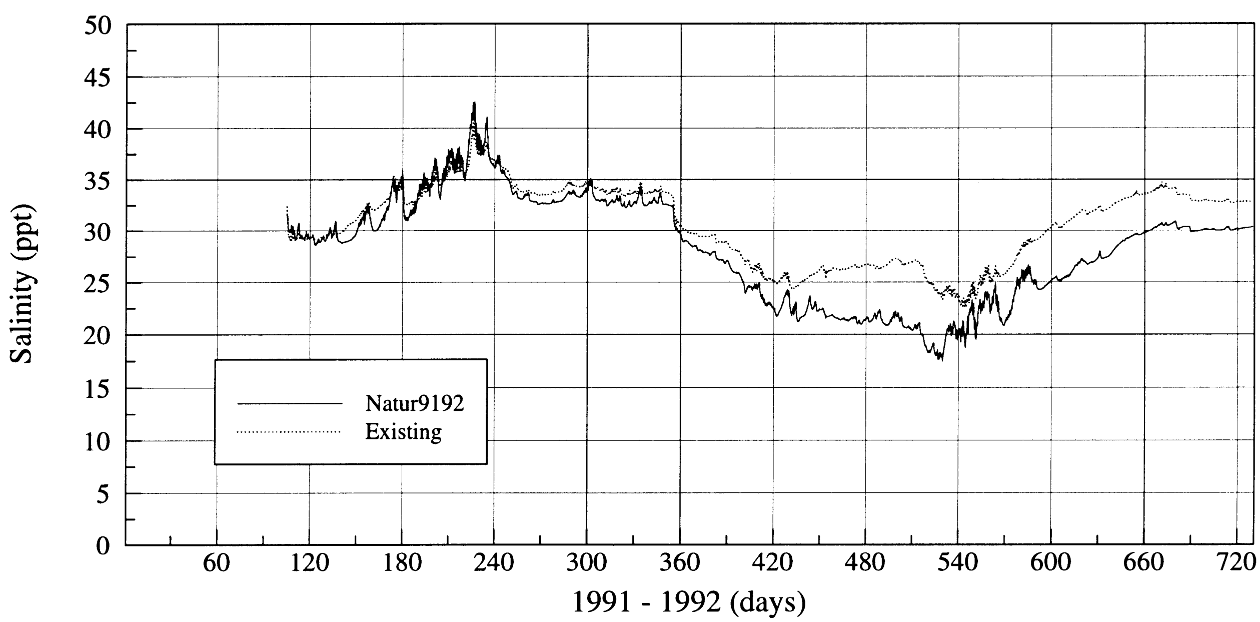

Figure IV.30 Simulated salinities in 1991-1992 for the existing condition and for the all impacts removed scenario

(e) Baffin Bay

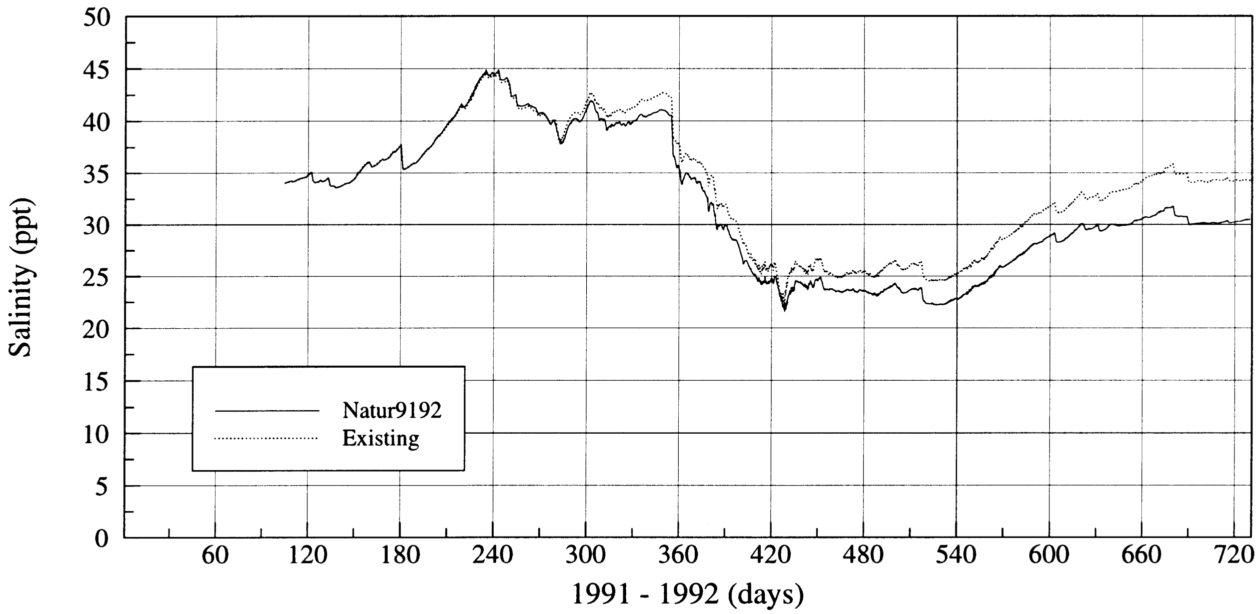

(f) GIWW near Pita Island

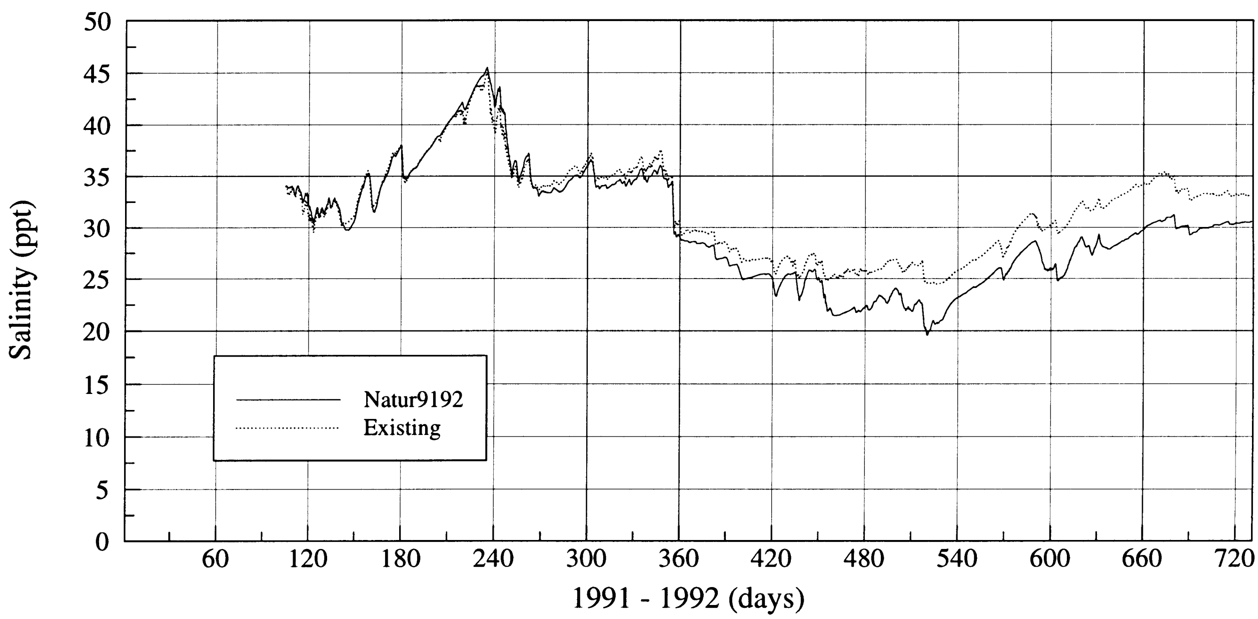

Figure 4.30 Simulated salinities in 1991-1992 for the existing condition and for the all impacts removed scenario

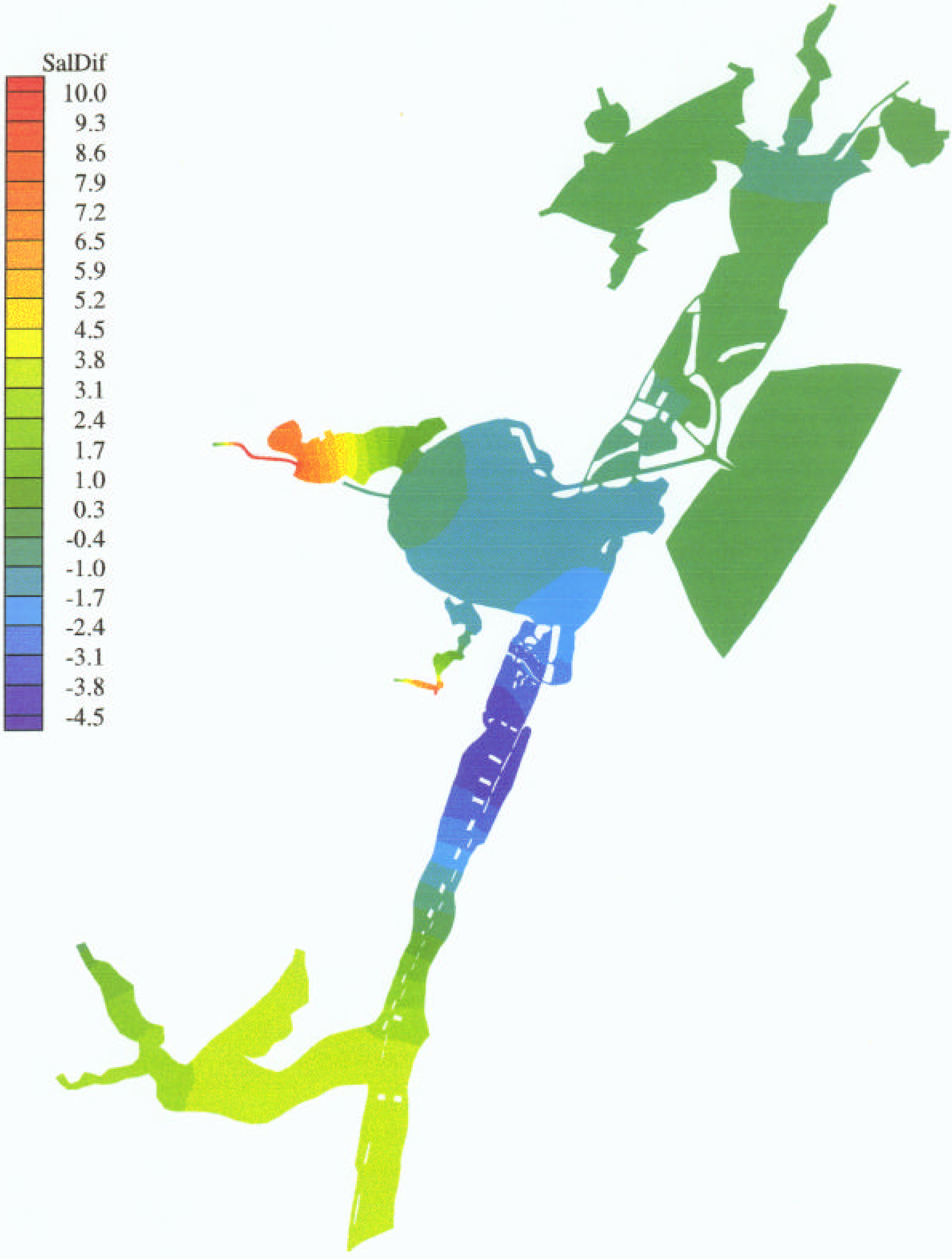

Figure IV.31 Salinity differences (ppt) in August 1989 between the existing condition and the all impacts removed case

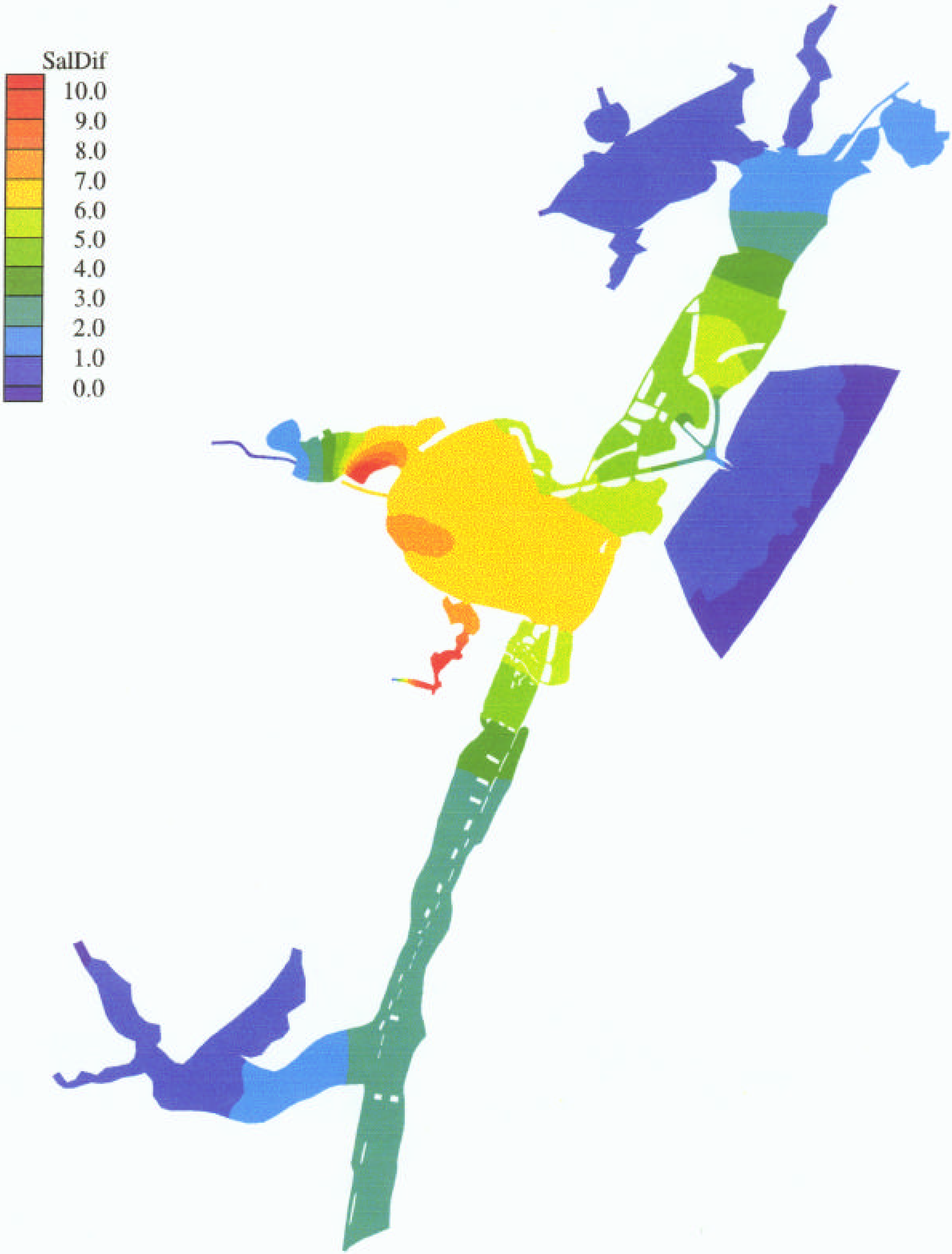

Figure IV.32 Salinity differences (ppt) in May 1992 between the existing condition and all impacts removed case

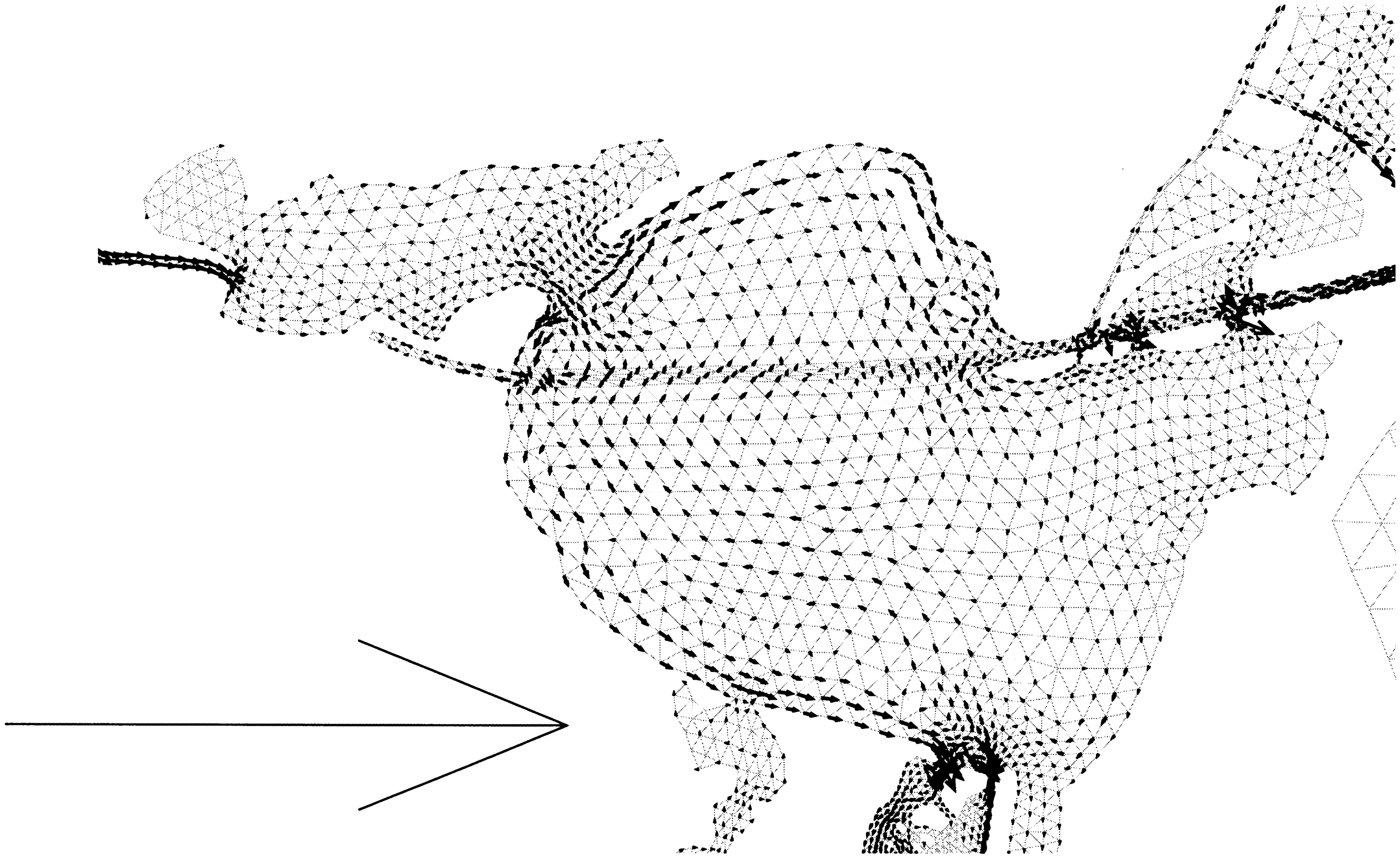

Figure IV.33 Residual vectors in Corpus Christi Bay and surrounding area for the all impacts removed scenario; the reference vector represents 1 fps

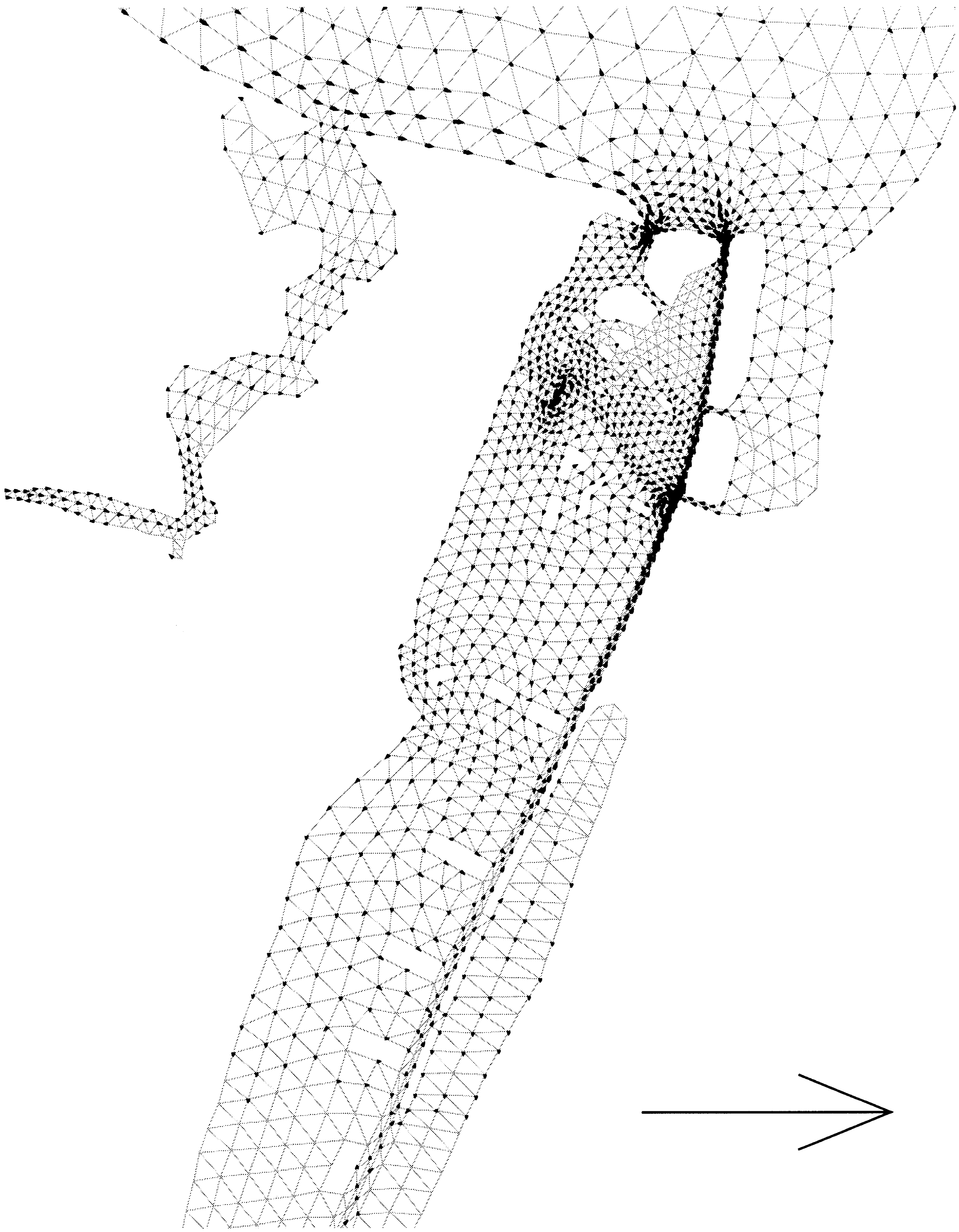

Figure IV.34 Residual vectors in Laguna Madre and Oso Bay for the all impacts removed scenario; the reference vector represents 1 fps

Figure IV.35 Flow traces for the all impacts removed case

Table of Contents

V. CONCLUSIONS

The effect of practices and structures on the circulation and salinity patterns in the Corpus Christi Bay National Estuary Program area was studied by means of computer model simulation. The practices included the withdrawal of seawater for power plant operation and the diversion of freshwater from the Nueces River for municipal and industrial use; structures included the JFK Causeway and Corpus Christi Ship Channel. The analysis was based on comparisons between the existing condition and simulations of scenarios in which the practices or structures were removed. Under each scenario two simulations of approximately two years duration were run: 1988 through 1989 for a dry period, and 1991 through 1992 for a wet period. Conclusions are as follows.

1. Circulation of bay water generated by withdrawal and discharge by power plants had an equalizing effect on the salinity. During the wet period of 1992 the salinity was estimated to be lower by as much as 6‰ in mid Nueces Bay, and by 2‰ in Corpus Christi Bay. During the dry period of 1989, salinity in Nueces Bay would have been higher without power plant operation, but by no more than 1‰, and the salinity in Corpus Christi Bay would not would have been affected significantly. The extent of the salinity change in Nueces Bay was limited to the area close to the power plant discharge and was not evident over a wide area of the bay.

In the Laguna Madre near the JFK Causeway, salinity would have been about 2‰ lower without power plant operation in the 1992 wet period, and 2 to 3‰ higher during the dry period of 1989. Pumping water from Laguna Madre through the power plant and into Oso Bay drew water into the upper Laguna Madre from Corpus Christi Bay. Corpus Christi Bay water was either higher or lower salinity than upper Laguna Madre water which often ameliorated Laguna Madre salinity. Cooling water withdrawal affected salinity in a large area of Laguna Madre, from just north of Baffin Bay to the JFK Causeway.

Under the existing condition the net flow analysis indicated that Corpus Christi Ship Channel carried water to the Nueces Bay Power Plant. This water returned to Corpus Christi Bay under the Nueces Causeway, then moved along the north shore of the bay and rejoined the ship channel near Ingleside. Net flow also traveled south from the head of the ship channel, along the west and south shore of Corpus Christi Bay and entered into Laguna Madre through the pass near the Naval Air Station and through the GIWW. It moved farther south through the Humble Channel and the GIWW at JFK Causeway toward the Barney Davis Power Plant. Then, as the water was withdrawn by the power plant near Pita Island and discharged to Oso Bay, the net flow moved through Oso Bay toward Corpus Christi Bay. Another loop was formed from the head of the ship channel toward mid Corpus Christi Bay south of the ship channel. It rejoined the ship channel near Ingleside. Thus two loops were formed, one on the north side and one on the south side of the ship channel.

2. If the water diverted from the Nueces River were returned to Nueces Bay, salinity at mid bay would have been consistently reduced by 1 to 2‰. The effect of returning diverted water was

widespread in Nueces Bay, with salinities reduced by 0 to 7‰ depending upon location. The return of diverted river flow would not have lowered the salinity in Corpus Christi Bay noticeably, nor would there have been an effect in Laguna Madre. A word of caution is necessary concerning this conclusion. The methodology for generating the comparison in this scenario assumed that river flow diverted at Calallen would have been transported to Nueces Bay. This presupposes the existence and release of water from the reservoirs upstream on the Nueces River. The water that was released and diverted downstream may have come from supplies that were impounded months or years before their release, especially during dry periods. If the reservoirs were not present it is possible that there would have been little or no natural river flow during dry periods. Thus, the results of this scenario may not be indicative of the salinity characteristics of the bay if the reservoirs had not been built and placed into operation.

3. If the JFK Causeway were removed, the flow through the same area would have increased slightly, about 4%, but salinity would not have been much different from the existing condition. Two areas would have been slightly affected by the removal, the upper Laguna Madre immediately adjacent to the JFK Causeway and Oso Bay. Salinities would have been slightly higher in the Causeway area if the structure had been removed and salinities in Oso Bay would also have been higher. The 0.2 to 0.5‰ increase in Oso Bay salinity would have been the result of the Barney Davis Power Plant pumping water of slightly higher salinity from the Laguna Madre into Oso Bay.

4. If the Corpus Christi Channel were removed, volume of tidal flow would have been reduced to one-fourth of current level at the Entrance Channel, to one-sixth of current level at the Corpus Christi Channel near Brown & Root, to one-third of current level at the Nueces Causeway, and by half at Lydia Ann Channel. The reduction would have been half or less at channels in the Laguna Madre.

The reduced tidal exchange would have prolonged the salinity conditions brought on by meteorological regimes; the lower salinity condition would have stayed low longer and the higher salinity condition would have stayed high longer. Salinity differences would have been 1 to 3‰ in Corpus Christi Bay, 1.5 to 3.5‰ in Nueces Bay, 1.5 to 2.5‰ in the JFK Causeway area. The extent of the effect of removal of the Corpus Christi Ship Channel would have been detectable throughout the study area. The greatest effect would have occurred in waterbodies close to the channel, but there would have been a detectable effect as far away as Baffin Bay. Of the four scenarios where individual structures or practices are removed, this is the only one where there was a detectable change in salinity in the bays of the northern part of the study area. Salinity would have tended to be slightly lower in Aransas Bay if the ship channel were removed.

5. If all impacts were removed together, the compound effects would have been strongest in Nueces Bay, which might have experienced salinities as much as 12‰ lower during wet periods and as much as 4‰ lower (not higher) during dry periods. The upper end of the bay near the

river mouth would have experienced the greatest salinity reduction. Salinity in Corpus Christi Bay would have been lower by as much as 6‰ during wet periods and higher by as much as 1.5‰ in dry periods.

Similarly, the salinity at the JFK Causeway area would have been lowered by as much as 5‰ during wet periods and as much as 4‰ higher during dry periods. The Naval Air Station and Pita Island sites showed the same pattern of salinity change as the JFK site. The removal of the ship channel appeared to have the greatest influence on salinity change at these sites. Removal of cooling water withdrawal had only about half the effect of ship channel removal. At the Baffin Bay site, the effect of the no impact scenario was to generally lower salinity by as much as 3.5‰. As in the case of the JFK Causeway, the change in salinity of Baffin Bay appears to have been affected most by the removal of the ship channel. (It is possible that the Baffin Bay site was influenced by the boundary condition set at the south end, so this conclusion may not be trustworthy.)

The compound effect of removing all four structures and practices on the bays in the northern end of the study area was nearly the same as the effect of removing the ship channel alone. The effects of removing the JFK Causeway, not diverting Nueces River flow, and not withdrawing cooling water had essentially no effect on Aransas and Copano bays.

The net flow patterns under the 'all impacts removed' scenario were very different from those of existing condition. The magnitudes of net movement were also much smaller than those of the existing condition. Flow entered Nueces Bay through the channel under the Nueces Causeway and exited through shallow areas north and south of the channel. Flow then traveled along the north shore of Corpus Christi Bay. Near the south end of the Nueces Causeway, the net flow started moving south along the shore line, entered Laguna Madre through the pass near the Naval Air Station, and traveled further south through Humble Channel. Near Pita Island the net flow diminished, but the GIWW carried net flow back to Corpus Christi Bay.

Considering the impacts of structures and practices on the estuaries in the Corpus Christi National Estuary Program area, the ship channel had the greatest effect on water movement and salinity. Its effects were felt in the estuaries to the north and as far south as Baffin Bay. Of lower magnitude with respect to total area affected was the return of diverted water to Nueces Bay. While this practice had a big effect on Nueces Bay, the salinities of other nearby estuaries including Corpus Christi Bay were hardly affected by the diversion. The withdrawal of cooling water from the Laguna Madre for the Barney Davis Power Plant was next on the magnitude scale. The area of the upper Laguna Madre affected by the withdrawal was greater than the area of Nueces Bay, but the salinity change tended to be much smaller than that caused by the river diversion. JFK Causeway had an even smaller effect on water movement and salinity. Its impact was largely limited to the area close to the causeway. The effects of the cooling water withdrawal and return on Nueces Bay and Corpus Christi Bay from the Nueces Bay Power Plant were localized and of small magnitude except during a very wet period.

This page intentionally left blank.

Table of Contents

VI. REFERENCES

Brandes, R.J., Masch, F.D. 1971. Tidal Hydrodynamic and Salinity Models for San Antonio and Matagorda Bays, Texas, F.D. Masch and Associates, Austin, TX.

Brandes, R.J., Masch, F.D. 1972. Tidal Hydrodynamic and Salinity Models for Coastal Bays--Evaporation Considerations, F.D. Masch and Associates, Austin, TX.

Brown, C.A., Militello, A., Kraus, N.C. 1995. Hydrodynamic Assessment for Elevation of the J.F.K. Causeway, Corpus Christi, Texas, Conrad Blucher Institute for Surveying and Science, Texas A&M University-Corpus Christi.

Carey, G.F. and Oden, J.T. 1986. '*Finite Elements: Fluid Mechanics*' Vol. VI, Prentice-Hall.

Duke, J.H. 1990. Upper Laguna Madre Modeling Study in the Vicinity of the John F. Kennedy Causeway, Corpus Christi, Texas. Austin, TX.

Kinmark, I.P.E. 1986. '*The Shallow Water Equations: Formulation, Analysis, and Application'*, Lecture Notes in Engineering, Springer-Verlag, 15.

Kolar, R.L., Gray, W.G., Westerink, J.J. 1992. ' An Analysis of Mass Conserving Properties of the Generalized Wave Continuity Equation' *Computational Methods in Water Resources IX*, Russell et al (eds) Computational Mechanics Publications/Elsevier Applied Science, 537-544.

Longley, W.L., ed. 1994. Freshwater Inflows to Texas Bays and Estuaries: Ecological Relationships and Methods for Determination of Needs. Prepared by Texas Water Development Board and Texas Parks and Wildlife Department. Published by Texas Water Development Board, Austin, TX.

Lynch, D.R., and Gray, W.G. 1979. 'A Wave Equation Model for Finite Element Tidal Computations' *Computers and Fluids*, 7, 3:207-228.

Matsumoto, J. 1992. User's manual for the Texas Water Development Board's Rainfall-Runoff Model, TxRR. Texas Water Development Board, Austin, TX.

Matsumoto, J. 1993. User's manual for the Texas Water Development Board's hydrodynamic and salinity model, TxBLEND. Texas Water Development Board, Austin, TX.

McArthur, K.E., 1996. 'Comparison of Finite Difference and Finite Element Hydrodynamic Models Applied to the Laguna Madre Estuary, Texas', Master Thesis, Department of Civil Engineering, Texas A&M University.

Pinder, G.F. and Gray W.G. 1977. *'Finite Element Simulation in Surface and Subsurface Hydrology'* Academic Press.

Texas Department of Water Resources. 1981. Nueces and Mission-Aransas Estuaries: A study of Influence of Freshwater Inflows. LP-108. Austin, TX.

Solis, R.S., 1994. Calibration of a Circulation and Salinity Transport Model for Galveston Bay. Texas Water Development Board staff report, Austin, TX.

Solis, R.S. and Matsumoto, J. 1991. Simulation Analysis of Changes in FLow Exchange in the Upper Laguna Madre with Removal of Portions of the John F. Kennedy Causeway. Texas Water Development Board staff report. Austin, TX.

Texas Department of Water Resources. 1982. Nueces and Mission-Aransas Estuaries: An Analysis of Bay Segment Boundaries, Physical Characteristics, and Nutrient Nrocesses. LP-83. Austin, TX.

Texas Water Development Board. 1967. Monthly Reservoir Evaporation Rates for Texas, 1940 through 1965. Austin, TX.

Whitledge, T.E. 1993. Enhanced Hydrographic Survey for CPL Discharge in Nueces Bay, Marine Science Institute, The University of Texas at Austin, Port Aransas, TX.

APPENDIX I. TxBLEND MODEL

TxBLEND is a two dimesional finite element model for simulating water circulation and salinity conditions in estuaries, based on the generalized wave continuity equation (Lynch and Gray 1979, Kinmark 1986, Kolar et al 1992) with linear triangular elements. TxBLEND is also capable of simulating an inundation and dewatering or wetting and drying process. There are three major partial differential equations solved numerically by the model. They are the continuity equation, the momentum equation, and the convective-diffusion equation or the conservative transport equation. The following explains how these equations are solved. A complete description of the model can be found in the user's manual (Matsumoto 1993).

Continuity Equation

The generalized wave continuity equation can be written as (Kinnmark 1986, Kolar et al 1992)

$$\frac{\partial^2\zeta}{\partial t^2} + G\frac{\partial\zeta}{\partial t} - \nabla\bullet\left\{\nabla\bullet(H\mathbf{VV}) + gH\nabla\zeta + \frac{gH^2}{2\rho}\nabla\rho + \mathbf{f}\times H\mathbf{V} - H\mathbf{A}\right\}$$
$$+(G-\tau)\nabla\bullet(H\mathbf{V}) - H\mathbf{V}\bullet\nabla\tau = G\cdot(r-e) \qquad \text{(A.1)}$$

where ζ is the water surface elevation above reference level; H is the total depth and equal to $h+\zeta$, h is the bathymetry; $\boldsymbol{V}$ is the velocity vector consisting of u and v; u is the x-component velocity; v is the y-component velocity; g is the gravitational accelaration; ρ is the density; f is the Coriolis parameter; τ is the bottom friction parameter--computed by $(g\cdot n^2\cdot\sqrt{u^2+v^2})/(2.208\cdot H^{4/3})$; n is Manning's roughness coefficient; $\boldsymbol{A}$ represents the wind stress vector consisting of A_x and A_y, where $A_x = (K\cdot V_w^2\cdot\cos\alpha)/H$ and $A_y = (K\cdot V_w^2\cdot\sin\alpha)/H$, in which K is the wind stress coefficient; V_w is the wind speed; α is the wind direction; r is the precipitation; and e is the evaporation. The parameter G in (A.1) is referred to as bigG in TxBLEND. This is a nonphysical parameter and represents the degree by which the primitive continuity equation is reflected in the wave continuity equation. The larger the bigG, the more the primitive continuity equation is incorporated, but also the more the oscillative nature of the primitive equation is manifest. The smaller the bigG, the smoother the solution may become, but enforcement of continuity may become weaker. The actual value of bigG depends on the application and is usually determined by test runs.

In TxBLEND the nonlinear term in the wave continuity equation is assumed negligible. The weighted residual form of Equation (A.1) becomes

$$\int_\Omega \left(\frac{\partial^2\zeta}{\partial t^2} + G\frac{\partial\zeta}{\partial t}\right)\cdot\phi_i\cdot dA + \int_\Omega \left(gH\nabla\zeta + \frac{gH^2}{2\rho}\nabla\rho + \mathbf{f}\times H\mathbf{V} - H\mathbf{A}\right)\cdot\nabla\phi_i\cdot dA$$
$$+\int_\Omega \{(G-\tau)\nabla\bullet(H\mathbf{V}) - H\mathbf{V}\bullet\nabla\tau\}\cdot\phi_i\cdot dA = -\int_\Gamma \left(\frac{\partial H\mathbf{V}}{\partial t} + \tau H\mathbf{V}\right)\bullet\mathbf{n}\phi_i\, ds \qquad \text{(A.2)}$$

where Ω represents the domain, Γ the boundary, and ϕ_i is the basis function for a linear triangular element--expressed as $\phi_i = a_i + b_i x + c_i y$ (Pinder and Gray 1977). The second integral in (A.2) is the gravity term to which Green's formula for integration by parts was applied to reduce the second order derivative to first order derivative. The right hand side of (A.2) is the boundary integral which is zero except at an inflow point where it is evaluated by $0.5\cdot(\partial Q/\partial t + \tau Q)$. After spatial discretization, the numerical equation can be written for node-*i* of element-*e* consisting of nodes *i*, *j*, and *k* as

$$\sum_{e\in EL_i}\left(\frac{\partial^2\zeta}{\partial t^2} + G\frac{\partial\zeta}{\partial t}\right)\frac{A_e}{3} + (Gravity) + \sum_{e\in EL_i}\{(G-\tau)_i\ (DQXDX_e + DQXDY_e\}\frac{A_e}{3}$$
$$-\sum_{e\in EL_i}\left(DTAUDX_e\cdot QX_i + DTAUDY_e\cdot QY_i\right)\frac{A_e}{3} = 0 \qquad \text{(A.3)}$$

where A_e is the element area, EL_i is the set containing the element number surrounding node *i*, $DQXDX_e$, etc. represent the computed values for $\partial q_x/\partial x$, etc. (note $Hu = q_x$). In (A.3) the time derivative term is lumped and the gravity term is treated specially. The gravity term is divided into two parts (Lynch and Gray, 1979), one associated with the bathymetry and the other with the water surface elevation:

$$gH\nabla\zeta \approx w\cdot gH_{t+\Delta t}\cdot\nabla\zeta_{t+\Delta t} + (1-w)\cdot gH_t\cdot\nabla\zeta_t$$
$$= w\cdot gh\cdot\nabla\zeta_{t+\Delta t} + w\cdot g\zeta_{t+\Delta t}\cdot\nabla\zeta_{t+\Delta t} + (1-w)\cdot g(h+\zeta)_t\cdot\nabla\zeta_t \qquad \text{(A.4)}$$

where *w* represents the weight, 1 being a totally implicit scheme; *t* is the current time level and $t+\Delta t$ is the future time level. The gravity term associated with the bathymetry is integrated as follows.

$$\int_\Omega gh\nabla\zeta\cdot\nabla\phi\ dA = \sum_{e\in EL_i}\int_{\Omega_e} gh\nabla\zeta\cdot\nabla\phi\ dA = \sum_{e\in EL_i}\int_{\Omega_e} gh\left(\frac{\partial\zeta}{\partial x}\frac{\partial\phi_i}{\partial x} + \frac{\partial\zeta}{\partial y}\frac{\partial\phi_i}{\partial y}\right)dA$$
$$\approx \sum_{e\in EL_i}\int_{\Omega_e} g\left(\sum_{j\in ND_e} h_j\phi_j\right)\left\{(\sum_{j\in ND_e}\zeta_j\ b_j)\cdot b_i + (\sum_{j\in ND_e}\zeta_j\ c_j)\cdot c_i\right\}dA$$
$$= \sum_{e\in EL_i} g\cdot smh_e\cdot\left\{(\sum_{j\in ND_e}\zeta_j\ b_j)\cdot b_i + (\sum_{j\in ND_e}\zeta_j\ c_j)\cdot c_i\right\}\frac{A_e}{3} \qquad \text{(A.5)}$$

where Ω_e represents the element *e*, ND_e is the set containing the node numbers that constitutes element *e*, and smh_e is the elemental sum of the bathymetries.

The time derivative term can be discretized by central differences as

$$(\zeta_{t+\Delta t} - 2\zeta_t + \zeta_{t-\Delta t}) / \Delta t^2 + G \cdot (\zeta_{t+\Delta t} - \zeta_{t-\Delta t}) / 2\Delta t \tag{A.6}$$

which is termed here the three-time level scheme. The two-time level scheme which is adopted in TxBLEND uses the present and future time levels for the first order derivative:

$$(\zeta_{t+\Delta t} - 2\zeta_t + \zeta_{t-\Delta t}) / \Delta t^2 + G \cdot (\zeta_{t+\Delta t} - \zeta_t) / \Delta t \tag{A.7}$$

Because TxBLEND internally iterates twice, the time derivative term can be positioned at the half time step into the future, $t + \Delta t / 2$, at the second internal iteration as in the two-time level scheme (A.7). This positioning improved the numerical accuracy and stability in test examples.

After multiplying (A.7) by Δt^2, the time derivative term and the gravity term of (A.5) associated with the water surface elevation of the future time level are combined to form the left hand side of the numerical equation. This is equivalent to the nonzero element of the coefficient matrix, expressed by

$$\left\{(1 + G \cdot \Delta t) + \Delta t^2 \cdot g \cdot smh_e \cdot (\, b_i b_j + c_i c_j)\right\} \frac{A_e}{3} \tag{A.8}$$

for the main diagonal element; for the off diagonal element, the $(1 + G \cdot \Delta t)$ term is dropped.

The remaining part of the gravity term and the time derivative term are shifted to the right hand side. They are:

$$\begin{aligned} &\left\{(2 + G \cdot \Delta t)\zeta_t - \zeta_{t-\Delta t}\right\} \frac{A_e}{3} - (1 - w)\Delta t^2 \cdot g \cdot smH_{e,t} \cdot (DZDX_e \cdot b_i + DZDY_e \cdot c_i)_t \cdot \frac{A_e}{3} \\ &\quad + w \cdot \Delta t^2 \cdot g \cdot smz_{e,t+\Delta t} \cdot (DZDX_e \cdot b_i + DZDY_e \cdot c_i)_{t+\Delta t} \cdot \frac{A_e}{3} \end{aligned} \tag{A.9}$$

where $smH_{e,t}$ is the elemental sum of total depths at time *t,* and $smz_{e,t+\Delta t}$ is the elemental sum of the water surface elevations at time $t + \Delta t$ --which are unknown, so approximations are used. The right-hand-side of the numerical equation for the wave continuity equation consists of the time derivative term and the gravity term as in (A.9) with the divergence term and the friction term which are the second and third summations in (A.3).

Notice the coefficient matrix is stationary because the nonzero elements (A.8) are stationary. One of the advantages of the wave continuity equation approach is the decoupling of the continuity equation and the momentum equation so that they can be solved sequentially, whereas in the primitive continuity equation they have to be solved simultaneously. Since the coefficient matrix is stationary, matrix inversion or matrix decomposition is required only once at the beginning of the simulation, which contributes to computational efficiency. As explained in the next section, the momentum equation is solved without matrix operation and thus as a whole the model is efficient from a computational point of view. (For a wet/dry version, the coefficient matrix is redecomposed whenever the dryness condition changes.)

Momentum Equation

The conservation form of the momentum equation for the x-direction can be expressed as

$$\frac{\partial q_x}{\partial t}+\frac{\partial u q_x}{\partial x}+\frac{\partial v q_x}{\partial y}+gH\frac{\partial \zeta}{\partial x}+\tau q_x = r_x \qquad \text{(A.10)}$$

where q_x is the unit flow in the x-direction, and r_x represents other terms shifted to the right hand side such as wind stress term and Coriolis term. The gravity term in (A.10) can be treated implicitly or explicitly by weighting the values at two time levels:

$$w\cdot(gH\cdot\partial\zeta/\partial x)_{t+\Delta t}+(1-w)\cdot(gH\cdot\partial\zeta/\partial x)_t \qquad \text{(A.11)}$$

where w=1 corresponds to a totally implicit scheme, w=0 to an explicit scheme, and w=0.5 to a Crank-Nicholson scheme. Because the continuity equation is solved seperately before the momentum equation, ζ at $t+\Delta t$ is available when the momentum equation is solved. Therefore the gravity terms for both current and future time levels are evaluated as if it were an explicit scheme.

The nonlinear terms are treated by the Picard iteration (Carey and Oden, 1986) in which there are two internal iterations at each time step. At the first internal iteration the solution is taken as an approximation to the future time level. For the second internal iteration the values at the half time step in the future can be approximated by

$$\zeta_{t+\Delta t/2}=(\zeta_t+\zeta^*_{t+\Delta t})/2 \quad \text{and} \quad q_{x,t+\Delta t/2}=(q_{x,t}+q^*_{x,t+\Delta t})/2 \qquad \text{(A.12)}$$

where the ones with * indicate solutions calculated in the first internal iteration. These values at the half time step are used for the nonlinear terms in the momentum equation and the divergence terms in the wave continuity equation. Notice that the two-time level scheme (A.7) for the first order time derivative is also positioned at the half time step in the future.

Using two time levels, the numerical equation for the momentum equation (A.10) can be written as

$$(q_{x,t+\Delta t}-q_{x,t})/\Delta t+0.5\cdot\left\{(\tau q_x)_{t+\Delta t}+(\tau q_x)_t\right\}=\bar{r}_x \qquad \text{(A.13)}$$

where $\bar{r}_x$ represents all the terms shifted to the right hand side. Then by rearrangement,

$$q_{x,t+\Delta t}=\left\{(1-0.5\cdot\tau_t)\cdot q_{x,t}+\Delta t\cdot\bar{r}_x\right\}/(1+0.5\cdot\Delta t\cdot\tau_{t+\Delta t}) \qquad \text{(A.14)}$$

where $\tau_{t+\Delta t}$ is the bottom friction factor at the future time level for which an approximation is used, which is calculated at the end of the first internal iteration.

Table of Contents To Top

Convective Diffusion Equation

The convective diffusion equation is expressed as

$$\frac{\partial C}{\partial t}+u\frac{\partial C}{\partial x}+v\frac{\partial C}{\partial y}-\frac{\partial}{\partial x}\left(D_x\frac{\partial C}{\partial x}\right)-\frac{\partial}{\partial y}\left(D_y\frac{\partial C}{\partial y}\right)=s \qquad \text{(A.15)}$$

where C is concentration or salinity, D_x and D_y are diffusion coefficients in the *x* direction and the *y* direction, and *s* is the source term. After applying Green's theorem to reduce the second order derivatives to the first order, the weighted residual form of Equation (A.15) becomes

$$\int_\Omega \frac{\partial C}{\partial t}\cdot\phi_i\cdot dA+\int_\Omega\left(u\frac{\partial C}{\partial x}+v\frac{\partial C}{\partial y}\right)\cdot\phi_i\cdot dA$$
$$+\int_\Omega\left(D_x\frac{\partial C}{\partial x}+D_y\frac{\partial C}{\partial y}\right)\cdot\nabla\phi_i\cdot dA=\int_\Omega s\cdot\phi_i\cdot dA \qquad \text{(A.16)}$$

Equation (A.16) is converted to a numerical equation by the finite element procedure. A fully implicit scheme is used to solve the system of equations in which the convective terms and the diffusion terms are treated implicitly. For an element *e* consisting of nodes *i*, *j*, and *k*, the nonzero element on the diagonal can be written as

$$\{1+\Delta t\cdot(\bar{u}_i\cdot b_i+\bar{v}_i\cdot c_i)+\Delta t\cdot(smD_x\cdot b_i\cdot b_i+smD_y\cdot c_i\cdot c_i)\}\cdot A_e/3 \qquad \text{(A.17)}$$

where the time derivative term is lumped, $\bar{u}_i$ and $\bar{v}_i$ are the weighted averages of *u* and *v*, and smD_x and smD_y are the elemental sums of diffusion coefficients. The weighted average is computed by $\bar{u}_i=(2\cdot u_i+u_j+u_k)/4$. For the off-diagonal nonzero elements, the equation is silmilar to (A.17) without the time derivative term. The contribution to the right-hand-side from node i of element e becomes $\bar{s}_i\cdot A_e/3$.